Available online at www.sciencedirect.com
SCIENCE DIRECT®
International Journal of Solids and Structures 42 (2005) 539–564
INTERNATIONAL JOURNAL OF SOLIDS and STRUCTURES
www.elsevier.com/locate/ijsolstr

Modeling and direct simulation of near-field granular flows

T.I. Zohdi *

Department of Mechanical Engineering, 6195 Etcheverry Hall, University of California, Berkeley, CA 94720-1740, USA

Received 9 April 2004
Available online 12 September 2004

Abstract

A wide range of modern applications have emerged where a successful analysis requires the simulation of flowing granular media which simultaneously incorporates near-field interaction between charged particles and intergranular contact. Such systems naturally arise in powder processing, micro- and nanotechnology, as well as in applications arising from the study of aerosols, epitaxy and astro- and geophysics. *The focus of this communication is to develop models and physically-based high-performance solution strategies for the direct rapid simulation of such flowing granular media.*

Keywords: Granular flow; Near-field effects; Direct simulation

1. Introduction

The study of granular media is wide ranging. Classical examples include the flow of "natural" materials such as sand and gravel associated with coastal erosion, landslides and avalanches. In this regard, as representative examples, we refer the reader to the extensive works of Hutter and collaborators: Tai et al. (2002, 2001a,b), Gray et al. (1999), Wieland et al. (1999), Berezin et al. (1998), Gray and Hutter (1997), Gray (2001), Hutter (1996), Hutter et al. (1995), Hutter and Rajagopal (1994), Koch et al. (1994), Greve and Hutter (1993) and Hutter et al. (1993), as well as the works of Behringer collaborators: Behringer (1993), Behringer and Baxter (1993), Behringer and Miller (1997) and Behringer et al. (1999). Man-made materials have been treated as well. [1] For general overviews we refer the reader to Jaeger and Nagel (1992a,b), Nagel (1992), Liu et al. (1991), Liu and Nagel (1993), Jaeger and Nagel (1993), Jaeger et al. (1994, 1996a,b, 1997).

* Tel.: +1 510 642 9172; fax: +1 510 642 5539.
E-mail address: zohdi@newton.berkeley.edu
[1] Over half (by weight) of the raw materials handled in chemical industries appear in granular form.

0020-7683/$ - see front matter
doi:10.1016/j.ijsolstr.2004.06.020

Recently, several modern applications, primarily driven by micro- and nanotechnology, have emerged where a successful analysis requires the simulation of flowing granular media involving simultaneous near-field interaction between charged particle, and momentum exchange through mechanical contact with friction between grains. For example, for many materials, flowing grains below the one millimeter scale can acquire relatively large electrostatic charges, leading to significant near-field forces between particles. [2] Charged material can lead to inconsistent "clean" manufacturing processes, for example, due to difficulties with dust control, although intentional charging of granular material can be quite useful in some application, for example involving electrostatic copiers, inkjet printers, powder coating machines, etc. The presence of near-field interaction forces can produce granular flows that are radically different than purely contact-driven scenarios. The determination of the dynamics of such materials is important for the accurate description of the flow of powders, which form the basis of nano- and microfabrication. Such near-field forces can lead to grain clustering, resulting in inconsistent fabrication quality. Clearly, neglecting such near-field effects can produce gross miscalculation of the power required to manipulate such flows. Thus, an issue of overriding importance to the successful description of such granular flows is the development of models and reliable techniques to rapidly computationally simulate the dynamics of multibody particulate systems involving near-field interaction and contact simultaneously. This is the focus of the present work.

2. Granular flow in the presence of near-fields

We treat the grains as spherical particles, i.e. their rotation with respect to their mass centers is deemed insignificant. [3] We consider a group of non-intersecting particles (n in total). The equations of motion, for the ith particle in a granular flow, is

$$m_i \ddot{\boldsymbol{r}}_i = \boldsymbol{\Psi}_i^{\text{tot}}(\boldsymbol{r}_1, \boldsymbol{r}_2, \ldots, \boldsymbol{r}_n), \tag{2.1}$$

where $\boldsymbol{r}_i$ is the position vector of the ith particle and where $\boldsymbol{\Psi}_i^{\text{tot}}$ represents all forces acting on particle i. In particular, $\boldsymbol{\Psi}_i^{\text{tot}} = \boldsymbol{\Psi}_i^{\text{nf}} + \boldsymbol{\Psi}_i^{\text{con}} + \boldsymbol{\Psi}_i^{\text{fric}}$ represents the forces due to near-field interaction, normal contact forces and friction. We consider the following relatively general central-force attraction–repulsion form for the near-field forces induced by all particles on particle i

$$\boldsymbol{\Psi}_i^{\text{nf}} = \sum_{j \neq i}^{n} \left(\left(\underbrace{\alpha_1 \|\boldsymbol{r}_i - \boldsymbol{r}_j\|^{-\beta_1}}_{\text{attraction}} - \underbrace{\alpha_2 \|\boldsymbol{r}_i - \boldsymbol{r}_j\|^{-\beta_2}}_{\text{repulsion}} \right) \underbrace{\boldsymbol{n}_{ij}}_{\text{unit vector}} \right), \tag{2.2}$$

where $\|\cdot\|$ represents the Euclidean norm in R^3, where all of the parameters, α's and β's, are non-negative, and where the normal direction is determined by the difference in the position vectors of the particles' centers, $\boldsymbol{n}_{ij} \stackrel{\text{def}}{=} \frac{\boldsymbol{r}_j - \boldsymbol{r}_i}{\|\boldsymbol{r}_i - \boldsymbol{r}_j\|}$.

2.1. Central-force properties

The force interaction of the form chosen is stable under certain conditions. We can consider stability to insure that, for small disturbances, the system will remain near an equilibrium position, whereas unstable

[2] For many engineering materials, some surface adhesion persists even when no explicit charging has occurred. For example, see Tabor (1975) or Johnson (1985).

[3] Henceforth, we use the term "grain" and "particle" interchangeably.

equilibrium will cause the system to move away from an equilibrium position, with an increasing velocity. Consider a potential function for a single particle, in one-dimensional motion, [4] attracted and repulsed from a point r_0 measured by the coordinate r,

$$V = \frac{\alpha_1}{-\beta_1 + 1} \mid r - r_0 \mid^{-\beta_1+1} - \frac{\alpha_2}{-\beta_2 + 1} \mid r - r_0 \mid^{-\beta_2+1}, \tag{2.3}$$

whose derivative produces the form of interaction forces introduced earlier:

$$\Psi^{\mathrm{nf}} = -\frac{\partial V}{\partial r} = (\alpha_1 \mid r - r_0 \mid^{-\beta_1} - \alpha_2 \mid r - r_0 \mid^{-\beta_2}) n, \tag{2.4}$$

where $n = \frac{r_0 - r}{|r - r_0|}$. For stability, we require

$$\frac{\partial^2 V}{\partial r^2} = -\alpha_1 \beta_1 \mid r - r_0 \mid^{-\beta_1 - 1} + \alpha_2 \beta_2 \mid r - r_0 \mid^{-\beta_2 - 1} > 0. \tag{2.5}$$

A static equilibrium point, $r = r_{\mathrm{e}}$, can be calculated by

$$\Psi^{\mathrm{nf}}(\mid r_{\mathrm{e}} - r_0 \mid) = -\alpha_1 \mid r_{\mathrm{e}} - r_0 \mid^{-\beta_1} + \alpha_2 \mid r_{\mathrm{e}} - r_0 \mid^{-\beta_2} = 0, \tag{2.6}$$

which implies

$$\mid r_{\mathrm{e}} - r_0 \mid = \left(\frac{\alpha_2}{\alpha_1} \right)^{\frac{1}{-\beta_1 + \beta_2}}. \tag{2.7}$$

Inserting Eq. (2.7) into Eq. (2.5) yields a restriction for stability

$$\frac{\beta_2}{\beta_1} > 1. \tag{2.8}$$

Further properties of this type of potential are given in Appendix A.

3. Mechanical contact with near-field interaction

We now consider cases where mechanical contact occurs between particles, in the presence of near-field interaction. A primary simplifying assumption is made: *the particles remain spherical after impact, i.e. any permanent deformation is negligible.* For two colliding particles i and j, normal to the line of impact, a statement for a balance of linear momentum relating the states before impact (time $= t$) and after impact (time $= t + \delta t$) reads as

$$m_i v_{i\mathrm{n}}(t) + m_j v_{j\mathrm{n}}(t) + \int_t^{t+\delta t} \boldsymbol{E}_i \cdot \boldsymbol{n}_{ij} \, \mathrm{d}t + \int_t^{t+\delta t} \boldsymbol{E}_j \cdot \boldsymbol{n}_{ij} \, \mathrm{d}t = m_i v_{i\mathrm{n}}(t + \delta t) + m_j v_{j\mathrm{n}}(t + \delta t), \tag{3.1}$$

where the subscript n denotes the normal component of the velocity (along the line connecting particle centers) and the $\boldsymbol{E}$'s represent all forces induced by near-field interaction with other particles, as well as all other external forces, if any, to the pair. If one isolates one of the members of the colliding pair, then

$$m_i v_{i\mathrm{n}}(t) + \int_t^{t+\delta t} I_{\mathrm{n}} \, \mathrm{d}t + \int_t^{t+\delta t} \boldsymbol{E}_i \cdot \boldsymbol{n}_{ij} \, \mathrm{d}t = m_i v_{i\mathrm{n}}(t + \delta t), \tag{3.2}$$

[4] Effectively, this is the motion in the normal direction, which is relevant for the central-force structure.

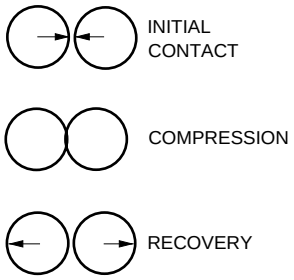

Fig. 1. Compression and recovery of two impacting particles.

where $\int_t^{t+\delta t} I_{\rm n}\,{\rm d}t$ is the total normal impulse due to impact. For a pair of particles undergoing impact, let us consider a decomposition of the collision event (Fig. 1) into a compression (δt_1) and recovery (δt_2) phase, i.e. $\delta t = \delta t_1 + \delta t_2$. Between the compression and recovery phases, the particles achieve a common velocity, [5] denoted $v_{\rm cn}$, at the intermediate time $t + \delta t_1$. We may write for particle i, along the normal, in the compression phase of impact

$$m_i v_{i\rm n}(t) + \int_t^{t+\delta t_1} I_{\rm n}\,{\rm d}t + \int_t^{t+\delta t_1} \boldsymbol{E}_i \cdot \boldsymbol{n}_{ij}\,{\rm d}t = m_i v_{\rm cn}, \tag{3.3}$$

and in the recovery phase

$$m_i v_{\rm cn} + \int_{t+\delta t_1}^{t+\delta t} I_n\,{\rm d}t + \int_{t+\delta t_1}^{t+\delta t} \boldsymbol{E}_i \cdot \boldsymbol{n}_{ij}\,{\rm d}t = m_i v_{i\rm n}(t+\delta t). \tag{3.4}$$

For the other particle (j), in the compression phase,

$$m_j v_{j\rm n}(t) - \int_t^{t+\delta t_1} I_{\rm n}\,{\rm d}t + \int_t^{t+\delta t_1} \boldsymbol{E}_j \cdot \boldsymbol{n}_{ij}\,{\rm d}t = m_j v_{\rm cn}, \tag{3.5}$$

and in the recovery phase

$$m_j v_{\rm cn} - \int_{t+\delta t_1}^{t+\delta t} I_n\,{\rm d}t + \int_{t+\delta t_1}^{t+\delta t} \boldsymbol{E}_j \cdot \boldsymbol{n}_{ij}\,{\rm d}t = m_j v_{j\rm n}(t+\delta t). \tag{3.6}$$

This leads to an expression for the coefficient of restitution

$$\begin{aligned} e \overset{\rm def}{=} \frac{\int_{t+\delta t_1}^{t+\delta t} I_n\,{\rm d}t}{\int_t^{t+\delta t_1} I_n\,{\rm d}t} &= \frac{m_i(v_{i\rm n}(t+\delta t) - v_{\rm cn}) - E_{i\rm n}(t+\delta t_1, t+\delta t)}{m_i(v_{\rm cn} - v_{i\rm n}(t)) - E_{i\rm n}(t, t+\delta t_1)} \\ &= \frac{-m_j(v_{j\rm n}(t+\delta t) - v_{\rm cn}) + E_{j\rm n}(t+\delta t_1, t+\delta t)}{-m_j(v_{\rm cn} - v_{j\rm n}(t)) + E_{j\rm n}(t, t+\delta t_1)}, \end{aligned} \tag{3.7}$$

[5] A common normal velocity for particles should be interpreted as indicating that the relative velocity in the normal direction between particle centers is zero.

where

$$
\begin{aligned}
E_{in}(t+\delta t_1, t+\delta t_2) &\stackrel{\text{def}}{=} \int_{t+\delta t_1}^{t+\delta t} \boldsymbol{E}_i \cdot \boldsymbol{n}_{ij}\, \mathrm{d}t, \\
E_{jn}(t+\delta t_1, t+\delta t_2) &\stackrel{\text{def}}{=} \int_{t+\delta t_1}^{t+\delta t} \boldsymbol{E}_j \cdot \boldsymbol{n}_{ij}\, \mathrm{d}t, \\
E_{in}(t, t+\delta t_1) &\stackrel{\text{def}}{=} \int_{t}^{t+\delta t_1} \boldsymbol{E}_i \cdot \boldsymbol{n}_{ij}\, \mathrm{d}t, \\
E_{jn}(t, t+\delta t_1) &\stackrel{\text{def}}{=} \int_{t}^{t+\delta t_1} \boldsymbol{E}_j \cdot \boldsymbol{n}_{ij}\, \mathrm{d}t.
\end{aligned}
\tag{3.8}
$$

If we eliminate v_{cn}, we obtain an expression for e

$$
e = \frac{v_{jn}(t+\delta t) - v_{in}(t+\delta t) + D_{ij}(t+\delta t_1, t+\delta t)}{v_{in}(t) - v_{jn}(t) + D_{ij}(t, t+\delta t_1)},
\tag{3.9}
$$

where [6]

$$
\begin{aligned}
D_{ij}(t+\delta t_1, t+\delta t) &\stackrel{\text{def}}{=} \frac{1}{m_i} E_{in}(t+\delta t_1, t+\delta t) - \frac{1}{m_j} E_{jn}(t+\delta t_1, t+\delta t), \\
D_{ij}(t, t+\delta t_1) &\stackrel{\text{def}}{=} \frac{1}{m_i} E_{in}(t, t+\delta t_1) - \frac{1}{m_j} E_{jn}(t, t+\delta t_1).
\end{aligned}
\tag{3.11}
$$

Thus, we may rewrite Eq. (3.9) as

$$
v_{jn}(t+\delta t) = v_{in}(t+\delta t) - D_{ij}(t+\delta t_1, t+\delta t) + e(v_{in}(t) - v_{jn}(t) + D_{ij}(t, t+\delta t_1)).
\tag{3.12}
$$

It is convenient to denote the average force acting on the particle from external sources as

$$
\overline{E}_{in} \stackrel{\text{def}}{=} \frac{1}{\delta t} \int_{t}^{t+\delta t} \boldsymbol{E}_i \cdot \boldsymbol{n}_{ij}\, \mathrm{d}t.
\tag{3.13}
$$

If e is explicitly known, then one can write, combining Eqs. (3.9) and (3.1)

$$
\begin{aligned}
v_{in}(t+\delta t) = {} & \frac{m_i v_{in}(t) + m_j (v_{jn}(t) - e(v_{in}(t) - v_{jn}(t)))}{m_i + m_j} \\
& + \frac{(\overline{E}_{in} + \overline{E}_{jn})\delta t - m_j (e D_{ij}(t, t+\delta t_1) - D_{ij}(t+\delta t_1, t+\delta t))}{m_i + m_j},
\end{aligned}
\tag{3.14}
$$

and, once $\boldsymbol{v}_{in}(t+\delta t)$ is known, one can subsequently also solve for $v_{jn}(t+\delta t)$ via Eq. (3.12).

Remark 1. Later, it will be useful to define the average impulsive normal contact force between the particles acting during the impact event as

$$
\overline{I}_{\mathrm{n}} \stackrel{\text{def}}{=} \frac{1}{\delta t} \int_{t}^{t+\delta t} I_{\mathrm{n}}\, \mathrm{d}t,
\tag{3.15}
$$

[6] This collapses to the classical expression for the ratio of the relative velocities before and after impact, if the near-field forces are negligible:

$$
e \stackrel{\text{def}}{=} \frac{v_{jn}(t+\delta t) - v_{in}(t+\delta t)}{v_{in}(t) - v_{jn}(t)}.
\tag{3.10}
$$

thus

$$\overline{I}_{\mathrm{n}} = \frac{m_i(v_{i\mathrm{n}}(t+\delta t) - v_{i\mathrm{n}}(t))}{\delta t} - \overline{E}_{i\mathrm{n}}. \tag{3.16}$$

In particular, as will be done later in the analysis, when we discretize the equations of motion with a discrete (finite difference) time step of Δt, where $\delta t \ll \Delta t$, we shall define the impulsive normal contact contribution to the total force (Eq. (2.1)) to be

$$\boldsymbol{\Psi}^{\mathrm{con}} = \frac{\overline{I}_{\mathrm{n}}\delta t}{\Delta t}\boldsymbol{n}_{ij}, \tag{3.17}$$

which will be included in the total force acting on a particle, $\boldsymbol{\Psi}_i^{\mathrm{tot}} = \boldsymbol{\Psi}_i^{\mathrm{nf}} + \boldsymbol{\Psi}_i^{\mathrm{con}} + \boldsymbol{\Psi}_i^{\mathrm{fric}}$.

Remark 2. At the implementation level, [7] we choose $\delta t = \gamma \Delta t$, where $0 < \gamma \ll 1$. This immediately allows a definition for $\delta\ t_1$ and δt_2

$$\delta t_1 + \delta t_2 = \delta t_1 + e\,\delta t_1 = \delta t \Rightarrow \delta t_1 = \frac{\gamma \Delta t}{1+e}, \tag{3.18}$$

while $\delta t_2 = \frac{e\gamma\Delta t}{1+e}$. This is consistent with the fact that the recovery time of deformation tends toward zero for $e \to 0$ (no recovery, asymptotically plastic), and tends toward equalling the compression time (δt_1) as $e \to 1$ (asymptotically elastic). If $e = 1$, there is no loss in energy, while if $e = 0$ there is a maximum loss in energy.

4. Kinetic energy dissipation

Consider two identical particles approaching one another, in the absence of near-field interaction. One can immediately write for the kinetic energy (T) before and after impact

$$T(t+\delta t) - T(t) = T(t)(e^2 - 1) \leqslant 0, \tag{4.1}$$

thus indicating the rather obvious fact that energy is lost with each subsequent impact for $e < 1$. Now consider a group of flowing particles, each with different velocities. We may decompose the velocity of each particle by ($\boldsymbol{v}_{\mathrm{cm}} = \frac{1}{M}\sum_{i=1}^{n} m_i \boldsymbol{v}_i$ and $M = \sum_{i=1}^{n} m_i$)

$$\boldsymbol{v}_i(t) = \boldsymbol{v}_{\mathrm{cm}}(t) + \delta \boldsymbol{v}_i(t), \tag{4.2}$$

where $\boldsymbol{v}_{\mathrm{cm}}(t)$ is the mean velocity of the group of particles and $\delta \boldsymbol{v}_i(t)$ is a purely fluctuating part of the velocity. For the entire group of particles at time $= t$

$$\begin{aligned}\sum_{i=1}^{n} m_i \boldsymbol{v}_i(t) \cdot \boldsymbol{v}_i(t) &= \sum_{i=1}^{n} m_i (\boldsymbol{v}_{\mathrm{cm}}(t) + \delta \boldsymbol{v}_i(t)) \cdot (\boldsymbol{v}_{\mathrm{cm}}(t) + \delta \boldsymbol{v}_i(t)) \\ &= M \boldsymbol{v}_{\mathrm{cm}}(t) \cdot \boldsymbol{v}_{\mathrm{cm}}(t) + 2\boldsymbol{v}_{\mathrm{cm}}(t) \cdot \underbrace{\sum_{i=1}^{n} m_i \delta \boldsymbol{v}_i(t)}_{=\boldsymbol{0}} + \sum_{i=1}^{n} m_i \delta \boldsymbol{v}_i(t) \cdot \delta \boldsymbol{v}_i(t).\end{aligned} \tag{4.3}$$

For any later stage, the mean velocity ($\boldsymbol{v}_{\mathrm{cm}}$) remains constant, and we have

$$\sum_{i=1}^{n} m_i (\boldsymbol{v}_i(t+\delta t) \cdot \boldsymbol{v}_i(t+\delta t)) = M \boldsymbol{v}_{\mathrm{cm}}(t) \cdot \boldsymbol{v}_{\mathrm{cm}}(t) + \sum_{i=1}^{n} m_i \delta \boldsymbol{v}_i(t+\delta t) \cdot \delta \boldsymbol{v}_i(t+\delta t). \tag{4.4}$$

[7] A typical choice is $0.001 \leqslant \gamma \leqslant 0.01$.

Subtracting Eq. (4.4) from Eq. (4.3) yields

$$\begin{aligned}
&\sum_{i=1}^{n} m_i \boldsymbol{v}_i(t+\delta t)\cdot \boldsymbol{v}_i(t+\delta t) - \sum_{i=1}^{n} m_i \boldsymbol{v}_i(t)\cdot \boldsymbol{v}_i(t)\\
&= \sum_{i=1}^{n} m_i \delta\boldsymbol{v}_i(t+\delta t)\cdot \delta\boldsymbol{v}_i(t+\delta t) - \sum_{i=1}^{n} m_i \delta\boldsymbol{v}_{(}t)\cdot \delta\boldsymbol{v}_i(t)\\
&\geqslant e^2 \sum_{i=1}^{n} m_i \delta\boldsymbol{v}_i(t)\cdot \delta\boldsymbol{v}_i(t) - \sum_{i=1}^{n} m_i \delta\boldsymbol{v}_i(t)\cdot \delta\boldsymbol{v}_i(t)\\
&= (e^2-1)\sum_{i=1}^{n} m_i \delta\boldsymbol{v}_i(t)\cdot \delta\boldsymbol{v}_i(t)\\
&\geqslant (e^2-1)\sum_{i=1}^{n} m_i \boldsymbol{v}_i(t)\cdot \boldsymbol{v}_i(t),
\end{aligned} \tag{4.5}$$

where the first inequality arises due to the fact that not all particles will experience an impact from one stage to the next, and where the second inequality arises due to the fact that the perturbation's energy must be smaller than the total. Thus, *in the absence of near-field interaction*, we should expect

$$e^2 - 1 \leqslant \frac{T(t+\delta t) - T(t)}{T(t)} \leqslant 0. \tag{4.6}$$

Remark. In order to help characterize the overall behavior motion, it is advantageous to decompose the kinetic energy per unit mass into the bulk motion of the center of mass and the motion relative to the center of mass

$$\overline{T}(t) = \frac{T(t)}{M} = \underbrace{\frac{1}{2}\boldsymbol{v}_{\mathrm{cm}}(t)\cdot \boldsymbol{v}_{\mathrm{cm}}(t)}_{\stackrel{\mathrm{def}}{=} T_{\mathrm{b}}=\text{bulk motion energy}} + \underbrace{\frac{1}{2M}\sum\nolimits_{i=1}^{n} m_i \delta\boldsymbol{v}_i(t)\cdot \delta\boldsymbol{v}_i(t)}_{\stackrel{\mathrm{def}}{=} T_{\mathrm{r}}=\text{relative motion energy}}. \tag{4.7}$$

Clearly, the identification of "bulk" and "relative" parts is important in some applications, and this decomposition provides a natural way of characterizing the granular flow. [8] We note that the system momentum is conserved provided there are no external forces to the entire system. For values of $e < 1$ the relative motion will eventually "die out", *if no near-field forces are present.* Sometimes expressions of the form $\sum_{i=1}^{n} m_i \boldsymbol{v}_i \cdot \boldsymbol{v}_i - M\boldsymbol{v}_{\mathrm{cm}}\cdot \boldsymbol{v}_{\mathrm{cm}} = \sum_{i=1}^{n} m_i \delta\boldsymbol{v}_i \cdot \delta\boldsymbol{v}_i$ are termed "granular gas temperatures".

5. Incorporating friction

To incorporate frictional stick–slip phenomena during impact for a general particle pair (i and j), the tangential velocities at the beginning of the impact time interval, time $= t$, are computed by subtracting the relative normal velocity away from the total relative velocity:

$$\boldsymbol{v}_{jt}(t) - \boldsymbol{v}_{it}(t) = (\boldsymbol{v}_j(t) - \boldsymbol{v}_i(t)) - ((\boldsymbol{v}_j(t) - \boldsymbol{v}_i(t))\cdot \boldsymbol{n}_{ij})\boldsymbol{n}_{ij}. \tag{5.1}$$

One then writes the equation for tangential momentum change during impact for the ith particle

$$m_i v_{it}(t) - \overline{I}_{\mathrm{f}}\,\delta t + \overline{E}_{it}\,\delta t = m_i v_{\mathrm{ct}}, \tag{5.2}$$

[8] For example in mixing processes.

where the friction contribution is $\overline{I}_{\rm f} = \frac{1}{\delta t}\int_t^{t+\delta t} I_{\rm f}\,{\rm d}t$, where the total contributions from all other particles in the tangential direction ($\boldsymbol{t}$) are $\overline{E}_{it} = \frac{1}{\delta t}\int_t^{t+\delta t} \boldsymbol{E}_i \cdot \boldsymbol{t}\,{\rm d}t$ and where $v_{\rm ct}$ is the common tangential velocity of particles i and j in the tangential direction. [9] Similarly, for the jth particle we have

$$m_j v_{jt}(t) + \overline{I}_{\rm f}\,\delta t + \overline{E}_{jt}\,\delta t = m_j v_{\rm ct}. \tag{5.3}$$

There are two unknowns, $\overline{I}_{\rm f}$ and $v_{\rm ct}$. The main quantity of interest is $\overline{I}_{\rm f}$, which can be solved for

$$\overline{I}_{\rm f} = \frac{\left(\frac{\overline{E}_{it}}{m_i} - \frac{\overline{E}_{jt}}{m_j}\right)\delta t + v_{it}(t) - v_{jt}(t)}{\left(\frac{1}{m_i} + \frac{1}{m_j}\right)\delta t}. \tag{5.4}$$

Thus, consistent with stick–slip models of Coloumb friction, one first assumes no slip occurs. If $|\,\overline{I}_{\rm f}\,| > \mu_{\rm s}\,|\,\overline{I}_{\rm n}\,|$, where $\mu_{\rm s} \geqslant \mu_{\rm d}$ is the coefficient of *static* friction and $\mu_{\rm d}$ is the dynamic coefficient of friction, then slip must occur and a dynamic sliding friction model is used. If sliding occurs, the friction force is assumed to be proportional to the normal force and opposite to the direction of relative tangent motion, i.e.

$$\boldsymbol{\Psi}_i^{\rm fric} \stackrel{\rm def}{=} \mu_{\rm d}\|\boldsymbol{\Psi}^{\rm con}\|\frac{\boldsymbol{v}_{jt} - \boldsymbol{v}_{it}}{\|\boldsymbol{v}_{jt} - \boldsymbol{v}_{it}\|} = -\boldsymbol{\Psi}_j^{\rm fric}. \tag{5.5}$$

5.1. Limitations on friction coefficients

There are limitations on the friction coefficients for such models to make physical sense. For example, reconsider the simple case of two identical particles (Fig. 2), in the absence of near-field forces approaching one another with velocity $\boldsymbol{v}(t)$, which can be decomposed into normal and tangential components, $\boldsymbol{v}(t) = v_{\rm n}(t)\boldsymbol{e}_{\rm n} + v_{\rm t}(t)\boldsymbol{e}_{\rm t}$. Now consider the pre- and post-impact kinetic energy, which is identical for each of the particles, assuming sliding (dynamic friction)

$$T(t) = \tfrac{1}{2}m(v_{\rm n}(t)^2 + v_{\rm t}(t)^2) \tag{5.6}$$

and

$$T(t+\delta t) = \tfrac{1}{2}m(v_{\rm n}(t+\delta t)^2 + v_{\rm t}(t+\delta t)^2). \tag{5.7}$$

Assuming sliding takes place, for either particle, the impulse–momentum relation in the normal direction can be written as

$$m v_{\rm n}(t) + \int_t^{t+\delta t} I_{\rm n}\,{\rm d}t = m v_{\rm n}(t+\delta t) \tag{5.8}$$

and the tangential direction

$$m v_{\rm t}(t) - \int_t^{t+\delta t} \mu_{\rm d} I_{\rm n}\,{\rm d}t = m v_{\rm t}(t+\delta t). \tag{5.9}$$

For the normal direction

$$\int_t^{t+\delta t} I_{\rm n}\,{\rm d}t = m(v_{\rm n}(t+\delta t) - v_{\rm n}(t)) = -(1+e)m v_{\rm n}(t). \tag{5.10}$$

Substituting this relation into the conservation of momentum in the tangential direction, we have

$$v_{\rm t}(t+\delta t) = v_{\rm t}(t) - (1+e)v_{\rm n}(t)\mu_{\rm d}. \tag{5.11}$$

[9] They do not move relative to one another.

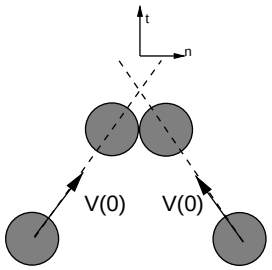

Fig. 2. Two identical particles approaching one another.

Now consider the restriction that the frictional forces cannot be so large that they reverse the initial tangential motion. Mathematically, this restriction can be written as $v_{\mathrm{t}}(t+\delta t) = v_{\mathrm{t}}(t) - (1+e)v_{\mathrm{n}}(t)\mu_{\mathrm{d}} \geqslant 0$, which leads to the following expression:

$$\mu_{\mathrm{d}} \leqslant \frac{v_{\mathrm{t}}(t)}{v_{\mathrm{n}}(t)(1+e)}. \tag{5.12}$$

Thus, the dynamic coefficient of friction must be restricted in order to make physical sense. Qualitatively, as e grows the restrictions on the coefficients of friction are more severe, although, the author has determined that, typically, values of $\mu_{\mathrm{d}} \leqslant 0.5$ usually are acceptable for the applications considered. For more general analyses on the existence and uniqueness of mechanical models involving friction see, for example, Oden and Pires (1983), Martins and Oden (1987), Kikuchi and Oden (1988), Klarbring (1990) or Cho and Barber (1999).

5.2. Velocity-dependent coefficients of restitution

It is important to realize that, in reality, the phenomenological parameter e depends on the severity of the impact velocity. For extensive experimental data, see Goldsmith (2001), or Johnson (1985) for a more detailed analytical treatment. Qualitatively, the coefficient of restitution has behavior as shown in Fig. 3. A mathematical idealization of the behavior can be constructed as follows:

$$e \stackrel{\mathrm{def}}{=} \max\left(e_0\left(1 - \frac{\Delta v_{\mathrm{n}}}{v^*}\right), e^-\right). \tag{5.13}$$

where v^* is a critical threshold velocity (normalization) parameter and where the relative velocity of approach is defined by $\Delta v_{\mathrm{n}} \stackrel{\mathrm{def}}{=} \mid v_{j\mathrm{n}}(t) - v_{i\mathrm{n}}(t) \mid$ and e^- is a lower limit to the coefficient of restitution.

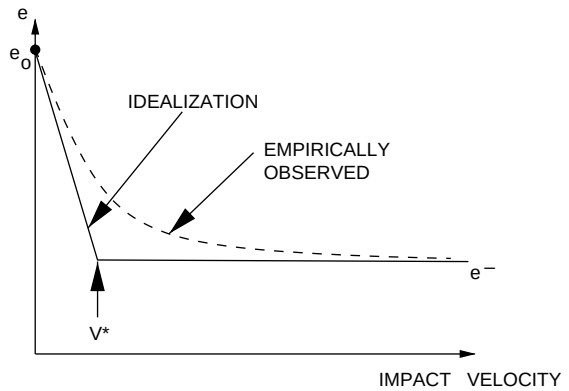

Fig. 3. Qualitative behavior of the coefficient of restitution with impact velocity.

Remark. In certain applications involving particle agglomeration in thermo-chemically reacting granular media, it is advantageous to construct coefficient of restitution relations that are pressure and temperature based, which include bonding as a limiting case as $e \rightarrow 0$. For example, development of ad hoc, empirically derived relations involving the material's Vicker's hardness and temperature to determine whether two particles bond can be found in Zohdi (2003a) and Zohdi (2003b), and are based on adhesion conditions developed in Nesterenko et al. (1994). See Meyers (1994) or Nesterenko (2001) for reviews on bonding criteria.

6. An iterative solution scheme

Implicit time-stepping methods, with time step size adaptivity, building on approaches found in Zohdi (2003b), will be used throughout the upcoming analysis. Accordingly, after time discretization of the acceleration term in the equations of motion (Eq. (2.1)) for a particle

$$\ddot{\boldsymbol{r}}_i^{L+1} \approx \frac{\boldsymbol{r}_i^{L+1} - 2\boldsymbol{r}_i^{L} + \boldsymbol{r}_i^{L-1}}{(\Delta t)^2}, \tag{6.1}$$

where, for brevity, we denote $\boldsymbol{r}_i^{L+1} \stackrel{\text{def}}{=} \boldsymbol{r}_i(t+\Delta t)$, $\boldsymbol{r}_i^{L} \stackrel{\text{def}}{=} \boldsymbol{r}_i(t)$, etc., one can arrive at the following abstract form, for the entire system, $\mathscr{A}(\boldsymbol{r}^{L+1}) = \mathscr{F}$. It is convenient to write

$$\mathscr{A}(\boldsymbol{r}^{L+1}) - \mathscr{F} = \mathscr{G}(\boldsymbol{r}^{L+1}) - \boldsymbol{r}^{L+1} + \mathscr{E} = \boldsymbol{0}, \tag{6.2}$$

where $\mathscr{E}$ is a remainder term which does not depend on the solution, i.e. $\mathscr{E} \neq \mathscr{E}(\boldsymbol{r}^{L+1})$. A straightforward iterative scheme can be written as

$$\boldsymbol{r}^{L+1,K} = \mathscr{G}(\boldsymbol{r}^{L+1,K-1}) + \mathscr{E}, \tag{6.3}$$

where $K = 1, 2, 3, \ldots$ is the index of iteration within time step $L+1$. The convergence of such a scheme is dependent on the behavior of $\mathscr{G}$. Namely, a sufficient condition for convergence is that $\mathscr{G}$ is a contraction mapping for all $\boldsymbol{r}^{L+1,K}$, $K = 1, 2, 3 \ldots$ In order to investigate this further, we define the error as $\varepsilon^{L+1,K} = \boldsymbol{r}^{L+1,K} - \boldsymbol{r}^{L+1}$. A necessary restriction for convergence is iterative self consistency, i.e. the exact solution must be represented by the scheme $\mathscr{G}(\boldsymbol{r}^{L+1}) + \mathscr{E} = \boldsymbol{r}^{L+1}$. Enforcing this restriction, a sufficient condition for convergence is the existence of a contraction mapping

$$\|\varepsilon^{L+1,K}\| = \|\boldsymbol{r}^{L+1,K} - \boldsymbol{r}^{L+1}\| = \|\mathscr{G}(\boldsymbol{r}^{L+1,K-1}) - \mathscr{G}(\boldsymbol{r}^{L+1})\| \leqslant \eta^{L+1,K}\|\boldsymbol{r}^{L+1,K-1} - \boldsymbol{r}^{L+1}\|, \tag{6.4}$$

where, if $\eta^{L+1,K} < 1$ for each iteration K, then $\varepsilon^{L+1,K} \rightarrow \boldsymbol{0}$ for any arbitrary starting value $\boldsymbol{r}^{L+1,K=0}$ as $K \rightarrow \infty$. The type of contraction condition discussed is sufficient, but not necessary, for convergence. In order to control convergence, we modify the discretization of the acceleration term: [10]

$$\ddot{\boldsymbol{r}}^{L+1} \approx \frac{\dot{\boldsymbol{r}}^{L+1} - \dot{\boldsymbol{r}}^{L}}{\Delta t} \approx \frac{\frac{\boldsymbol{r}^{L+1} - \boldsymbol{r}^{L}}{\Delta t} - \dot{\boldsymbol{r}}^{L}}{\Delta t} \approx \frac{\boldsymbol{r}^{L+1} - \boldsymbol{r}^{L}}{\Delta t^2} - \frac{\dot{\boldsymbol{r}}^{L}}{\Delta t}. \tag{6.5}$$

Inserting this into $m\ddot{\boldsymbol{r}} = \boldsymbol{\Psi}^{\text{tot}}(\boldsymbol{r})$ leads to

$$\boldsymbol{r}^{L+1,K} \approx \underbrace{\frac{\Delta t^2}{m}\left(\boldsymbol{\Psi}^{\text{tot}}(\boldsymbol{r}^{L+1,K-1})\right)}_{\mathscr{G}(\boldsymbol{r}^{L+1,K-1})} + \underbrace{\left(\boldsymbol{r}^{L} + \Delta t \dot{\boldsymbol{r}}^{L}\right)}_{\mathscr{E}}, \tag{6.6}$$

whose convergence is restricted by

[10] This collapses to a stencil of $\ddot{\boldsymbol{r}}^{L+1} = \frac{\boldsymbol{r}^{L+1} - 2\boldsymbol{r}^{L} + \boldsymbol{r}^{L-1}}{(\Delta t)^2}$, when the time step size is uniform.

$$\eta \propto \mathrm{EIG}(\mathscr{G}) \propto \frac{\Delta t^2}{m}. \tag{6.7}$$

Therefore, we see that the eigenvalues of $\mathscr{G}$ are (1) directly dependent on the strength of the interaction forces, (2) inversely proportional to the mass and (3) directly proportional to $(\Delta t)^2$. Therefore, if convergence is slow within a time step, the time step size, an adjustable parameter, can be reduced by an appropriate amount to increase the rate of convergence. Thus, decreasing the time step size improves the convergence, however, we want to simultaneously maximize the time-step sizes to decrease overall computing time, while still meeting an error tolerance. In order to achieve this goal, we follow an approach in Zohdi (2002) and Zohdi (2003b) originally developed for continuum thermo-chemical multifield problems in which (1) one approximates $\eta^{L+1,K} \approx S(\Delta t)^p$ (S is a constant) and (2) one approximates the error within an iteration to behave according to $(S(\Delta t)^p)^K \|\varepsilon^{L+1,0}\| = \|\varepsilon^{L+1,K}\|$, $K = 1, 2, \ldots$, where $\|\varepsilon^{L+1,0}\|$ is the initial norm of the iterative error and S is a function intrinsic to the system. [11] Our goal is to meet an error tolerance in exactly a preset number of iterations. To this end, one writes this in the following approximate form, $(S(\Delta t_{\mathrm{tol}})^p)^{K_{\mathrm{d}}} \|\varepsilon^{L+1,0}\| = \mathrm{TOL}$, where TOL is a tolerance and where K_{d} is the number of desired iterations. [12] If the error tolerance is not met in the desired number of iterations, the contraction constant $\eta^{L+1,K}$ is too large. Accordingly, one can solve for a new smaller step size, under the assumption that S is constant,

$$\Delta t_{\mathrm{tol}} = \Delta t \left(\frac{\left(\frac{\mathrm{TOL}}{\|\varepsilon^{L+1,0}\|} \right)^{\frac{1}{pK_d}}}{\left(\frac{\|\varepsilon^{L+1,K}\|}{\|\varepsilon^{L+1,0}\|} \right)^{\frac{1}{pK}}} \right). \tag{6.8}$$

The assumption that S is constant is not critical, since the time steps are to be recursively refined and unrefined repeatedly. Clearly, the expression in Eq. (6.8) can also be used for time step enlargement, if convergence is met in less than K_{d} iterations.

6.1. Observations

Remark 3. Time-step size adaptivity is paramount, since the flow's dynamics can dramatically change over the course of time, requiring radically different time step sizes for a preset level of accuracy. However, one must respect an upper bound dictated by the discretization error, i.e., $\Delta t \leqslant \Delta t^{\mathrm{lim}}$.

Remark 4. Classical solution methods require $\mathcal{O}(N^3)$ operations, whereas iterative schemes, such as the one presented, typically require order N^q, where $1 \leqslant q \leqslant 2$. For details see Axelsson (1994). Also, such solvers are highly advantageous since solutions to previous time steps can be used as the first guess to accelerate the solution procedure.

Remark 5. A recursive iterative scheme of Jacobi-type, where the updates are made only after one complete iteration, was illustrated here only for algebraic simplicity. The Jacobi method is easier to address theoretically, while the Gauss–Seidel type method, which involves immediately using the most current values, when they become available, is usually used at the implementation level. As is well-known that, under relatively general conditions, if the Jacobi method converges, the Gauss–Seidel method converges at a faster rate, while if the Jacobi method diverges, the Gauss–Seidel method diverges at a faster rate. For example, see Axelsson (1994). The iterative approach presented can also be considered as a type of staggering scheme. Staggering schemes have a long history in the computational mechanics community. For example,

[11] For the class of problems under consideration, due to the quadratic dependency on Δt, $p \approx 2$.

[12] Typically, K_{d} is chosen to be between 5 and 10 iterations.

see Park and Felippa (1983), Zienkiewicz (1984), Schrefler (1985), Lewis et al. (1992), Doltsinis (1993, 1997), Piperno (1997), Lewis and Schrefler (1998), Le Tallec and Mouro (2001) and Zohdi (2002, 2004).

Remark 6. It is important to realize the Jacobi method is perfectly parallelizable. In other words, the calculation for each particle are uncoupled, with the updates only coming afterward. Gauss–Seidel, since it requires the most current updates, couples the particle calculations immediately. However, these methods can be combined to create hybrid approaches, whereby the entire granular flow is partitioned into groups and within each group a Gauss–Seidel method is applied. In other words, for a group, the positions of any members from outside are initially frozen, as far as calculations involving members of the group are concerned. After each isolated group's solution (particle positions) has converged, computed in parallel, then all positions are updated, i.e. the most current positions become available to all members of the granular flow, and the isolated group calculations are repeated.

Remark 7. We observe that for the entire ensemble of members one has

$$\sum_{i=1}^{n} m_i \ddot{\boldsymbol{r}}_i = \sum_{i=1}^{n} \boldsymbol{\Psi}_i^{\text{tot}}(\boldsymbol{r}). \tag{6.9}$$

We may decompose the total force due to external sources and internal interaction, $\boldsymbol{\Psi}_i^{\text{tot}}(\boldsymbol{r}) = \boldsymbol{\Psi}_i^{\text{EXT}}(\boldsymbol{r}) + \boldsymbol{\Psi}_i^{\text{INT}}(\boldsymbol{r})$, to obtain

$$\sum_{i=1}^{n} m_i \ddot{\boldsymbol{r}}_i = \sum_{i=1}^{n} \left(\boldsymbol{\Psi}_i^{\text{EXT}}(\boldsymbol{r}) + \boldsymbol{\Psi}_i^{\text{INT}}(\boldsymbol{r}) \right) = \sum_{i=1}^{n} \boldsymbol{\Psi}_i^{\text{EXT}}(\boldsymbol{r}) + \underbrace{\sum_{i=1}^{n} \boldsymbol{\Psi}_i^{\text{INT}}(\boldsymbol{r})}_{=\boldsymbol{0}}. \tag{6.10}$$

Thus, a consistency check can be made by tracking the condition, $\| \sum_{i=1}^{n} \boldsymbol{\Psi}_i^{\text{INT}}(\boldsymbol{r}) \| = \boldsymbol{0}$. This condition is usually met to an extremely high degree by the temporally adaptive scheme introduced earlier. However, this is only a necessary condition, but not sufficient, for zero error.

Remark 8. The alternative solution scheme would be to attempt to compute the solution by applying a gradient-based scheme like Newton's method. For the class of systems under consideration, there are difficulties with such an approach. For example, consider the residual $\mathscr{R}^{L+1} \stackrel{\text{def}}{=} \mathscr{A}(\boldsymbol{r}^{L+1}) - \mathscr{F}$. Linearization leads to

$$\mathscr{R}(\boldsymbol{r}^{L+1,K}) = \mathscr{R}(\boldsymbol{r}^{L+1,K-1}) + (\nabla_{\boldsymbol{r}} \mathscr{R}(\boldsymbol{r}))|_{\boldsymbol{r}^{L+1,K}} (\boldsymbol{r}^{L+1,K} - \boldsymbol{r}^{L+1,K-1}) + \mathscr{O}(\|\Delta \boldsymbol{r}\|^2), \tag{6.11}$$

and thus the Newton updating scheme can be developed by enforcing $\mathscr{R}(\boldsymbol{r}^{L+1,K}) \approx \boldsymbol{0}$, leading to

$$\boldsymbol{r}^{L+1,K} = \boldsymbol{r}^{L+1,K-1} - (\mathscr{A}^{\text{TAN},L+1,K-1})^{-1} \mathscr{R}(\boldsymbol{r}^{L+1,K-1}), \tag{6.12}$$

where $\mathscr{A}^{\text{TAN},L+1,K-1} = (\nabla_{\boldsymbol{r}} \mathscr{A}(\boldsymbol{r}))|_{\boldsymbol{r}^{L+1,K-1}} = (\nabla_{\boldsymbol{r}} \mathscr{R}(\boldsymbol{r}))|_{\boldsymbol{r}^{L+1,K-1}}$, is the tangent. Therefore, one has a fixed-point operator of the form $\mathscr{G}(\boldsymbol{r}) = \boldsymbol{r} - (\mathscr{A}^{\text{TAN}})^{-1} \mathscr{R}(\boldsymbol{r})$. For the problems considered, it is unlikely that the gradients of $\mathscr{A}$ remain positive definite, or even that $\mathscr{A}$ is continuously differentiable, due to the impact events. Essentially, $\mathscr{A}$ will have non-convex and nondifferentiable dependence on the positions of the particles. Thus, a fundamental difficulty is the possibility of a zero or non-existent tangent ($\mathscr{A}^{\text{TAN}}$). Therefore, while Newton's method usually converges at a faster rate than a direct fixed point iteration, quadratic as opposed to superlinear, its range of applicability is less robust.

Remark 9. Convergence of an iterative scheme can sometimes be accelerated by *relaxation* methods. The basic idea in relaxation methods is to introduce a relaxation parameter, γ, into the iterations

$$\boldsymbol{r}^{L+1,K} = \gamma(\mathscr{G}(\boldsymbol{r}^{L+1,K-1}) + \mathscr{E}) + (1-\gamma)\boldsymbol{r}^{L+1,K-1}. \tag{6.13}$$

Since the scheme must reproduce the exact solution we have

$$\boldsymbol{r}^{L+1} = \gamma(\mathscr{G}(\boldsymbol{r}^{L+1}) + \mathscr{E}) + (1-\gamma)\boldsymbol{r}^{L+1}. \tag{6.14}$$

Subtracting Eq. (6.14) from Eq. (6.13) yields

$$\boldsymbol{r}^{L+1,K} - \boldsymbol{r}^{L+1} = \gamma(\mathscr{G}(\boldsymbol{r}^{L+1,K-1}) - \mathscr{G}(\boldsymbol{r}^{L+1})) + (1-\gamma)(\boldsymbol{r}^{L+1,K-1} - \boldsymbol{r}^{L+1}). \tag{6.15}$$

One then forms

$$\|\boldsymbol{r}^{L+1,K} - \boldsymbol{r}^{L+1}\| \leqslant \eta^{\gamma}\|\boldsymbol{r}^{L+1,K-1} - \boldsymbol{r}^{L+1}\|, \tag{6.16}$$

where the parameter γ is chosen such that $\eta^{\gamma} \leqslant \eta$, i.e. to induce faster convergence, relative to a relaxation-free approach. The primary difficulty is that the selection of such γ to induce faster convergence, if they exist, is unknown a-priori. For even the linear theory, i.e. when $\mathscr{G}$ is a linear operator, such parameters are unknown and are usually computed by empirical trial and error procedures. See Axelsson (1994) for reviews.

6.2. Algorithmic implementation

An implementation of the process is as follows:

(1) GLOBAL FIXED − POINT ITERATION : (SET i = 1 AND K = 0) :

(2) IF i > n THEN GO TO (4)

(3) IF i ≤ n THEN :

(a) COMPUTE POSITION : $\boldsymbol{r}_i^{L+1,K} = \dfrac{\Delta t^2}{m_i}\left(\boldsymbol{\Psi}_i^{tot}(\boldsymbol{r}^{L+1,K-1})\right) + \boldsymbol{r}_i^{L} + \Delta t\dot{\boldsymbol{r}}_i^{L}$

(b) GO TO (2) AND NEXT FLOW PARTICLE (i = i + 1)

(4) ERROR MEASURE :

(a) $\varepsilon_K \stackrel{\text{def}}{=} \dfrac{\sum_{i=1}^{n} ||\boldsymbol{r}_i^{L+1,K} - \boldsymbol{r}_i^{L+1,K-1}||}{\sum_{i=1}^{n} ||\boldsymbol{r}_i^{L+1,K}||}$

(b) $Z_K \stackrel{\text{def}}{=} \dfrac{\varepsilon_K}{TOL_r}$

(c) $\Phi_K \stackrel{\text{def}}{=} \left(\dfrac{(\frac{TOL}{\varepsilon_0})^{\frac{1}{pK_d}}}{(\frac{\varepsilon_K}{\varepsilon_0})^{\frac{1}{pK}}} \right)$

(5) IF TOLERANCE MET ($Z_K \leq 1$) AND $K < K_d$ THEN :

(a) CONSTRUCT NEW TIME STEP : $\Delta t = \Phi_K \Delta t$

(b) SELECT MINIMUM : $\Delta t = MIN(\Delta t^{lim}, \Delta t)$

(c) INCREMENT TIME : $t = t + \Delta t$ AND GO TO (1)

(6) IF TOLERANCE NOT MET ($Z_K > 1$) AND $K = K_d$ THEN :

(a) CONSTRUCT NEW TIME STEP : $\Delta t = \Phi_K \Delta t$

(b) RESTART AT TIME = t AND GO TO (1)

(6.17)

The overall goal is to deliver solutions where the iterative consistency error is controlled and the temporal discretization accuracy dictates the upper limits on the time step size ($\Delta t^{\lim}$).

7. Numerical simulation

In order to simulate a granular flow, we consider a group of n randomly positioned particles in a cube with dimensions $D \times D \times D$. During the simulation of groups of particles, if a particle escapes from the control volume, the position component is reversed and the same velocity component is retained (now incoming). Thus, for example, if the x component of the position vector exceeds the boundary of the control volume, then $r_{ix} = -r_{ix}$ is enforced. These are sometimes referred to as periodic boundary conditions. The particle size and volume fraction are determined by a particle/sample size ratio, which is defined via a subvolume size $V \stackrel{\text{def}}{=} \frac{D \times D \times D}{n}$, where n is the number of particles. [13] The ratio between the radius (b) and the subvolume are related by $\mathscr{L} \stackrel{\text{def}}{=} \frac{b}{V^{\frac{1}{3}}}$. The volume fraction occupied by the particles is $v_{\mathrm{f}} \stackrel{\text{def}}{=} \frac{4\pi\mathscr{L}^3}{3}$. Thus, the total volume occupied by the particles, denoted Δ, can be written as

$$\Delta = v_{\mathrm{f}} n V, \tag{7.1}$$

and the mass total mass $M = \sum_{i=1}^{n} m_i = \rho\Delta$, while that of an individual particle, assuming that all are the same size, is

$$m_i = \frac{\rho\Delta}{n} = \rho\frac{4}{3}\pi b_i^3. \tag{7.2}$$

7.1. Simulation parameters

The relevant simulation parameters were

- number of particles = 100,
- initial mean velocity field = (1.0, 0.1, 0.1) m/s,
- initial random perturbations around mean velocity = ($\pm$1.0, $\pm$0.1, $\pm$0.1) m/s,
- length scale of the particles, $\mathscr{L} = 0.25$, with corresponding volume fraction $v_{\mathrm{f}} = \frac{4\pi\mathscr{L}^3}{3} = 0.0655$ and radius $b = 0.0539$,
- mass density of the particles = 2000 kg/m^3,
- simulation duration = 1 s,
- initial time step size = 0.001 s,
- time step upper bound = 0.01 s.
- tolerance for the fixed-point iteration = 10^{-8}.

We introduce the following (per unit *mass*^{2}) decompositions for the key near-field parameters, for example for the force imparted on particle i by particle j and vice versa [14]

- $\alpha_{1ij} = \overline{\alpha}_1 m_i m_j$,
- $\alpha_{2ij} = \overline{\alpha}_2 m_i m_j$,

[13] D is normalized to unity in the simulations.

[14] Alternatively, if the near-fields are related to the amount of surface area, this scaling could be done per unit area.

The parameters $\overline{\alpha}_1$ and $\overline{\alpha}_2$, which represent the strength of the near-field interaction forces per unit *mass*^{2}, were varied to investigate the near-field effects on the overall granular flow. During the simulations, we enforced the stability condition in Eq. (2.8), by setting $(\beta_1, \beta_2) = (1, 2)$.

7.2. Results and observations

The starting configuration is shown in Fig. 4. Figs. 5 and 6 illustrate the computational results. The type of motion, characterized by the proportions of bulk and relative kinetic energy in the system is dramatically different with increasing severity of the near-field forces. [15] Notice that the kinetic energy per unit mass is non-monotone when the near-field interactions are taken into account (Fig. 6). One may observe from Fig. 5, that as the near-field strength is increased, the component of the kinetic energy corresponding to the relative motion does not decay, and actually becomes dominant with time. Essentially, the near-field interaction becomes strong enough that the purely flowing system experiences a transition to a *vibrating ensemble.* This transition can be qualitatively examined by recognizing that the governing equations are formally similar to classical, normalized, linear (or linearized) second order equations governing a one degree of freedom harmonic oscillator of the form

$$\ddot{r} + 2\zeta\omega_{\mathrm{n}}\dot{r} + \omega_{\mathrm{n}}^2 r = \frac{f(t)}{m}, \tag{7.3}$$

where $\omega_n = \sqrt{\frac{k}{m}}$, where r the position measured from equilibrium ($r = 0$), where k is the modulus of the restoring force (kr), where m represents the mass, where $\zeta = \frac{d}{2m\omega_{\mathrm{n}}}$, d being a constant of damping and where $f(t)$ is an external forcing term. The damped period of natural, *force-free*, vibration is $\mathscr{T}_{\mathrm{d}} \stackrel{\mathrm{def}}{=} \frac{2\pi}{\omega_{\mathrm{d}}}$, where $\omega_{\mathrm{d}} \stackrel{\mathrm{def}}{=} \omega_n\sqrt{1-\zeta^2}$ is the "damped natural frequency". Using standard procedures in differential equations, one performs the following decomposition into a homogeneous and particular part, $r = r_{\mathrm{H}} + r_{\mathrm{P}}$. The homogeneous part must satisfy $\ddot{r}_{\mathrm{H}} + 2\zeta\omega_{\mathrm{n}}\dot{r}_{\mathrm{H}} + \omega_{\mathrm{n}}^2 r_{\mathrm{H}} = 0$. Assuming the standard form $r_{\mathrm{H}} = \exp(\lambda t)$, which upon substitution into the governing equation yields $\lambda^2\exp(\lambda t) + 2\zeta\omega_{\mathrm{n}}\lambda\exp(\lambda t) + \omega_{\mathrm{n}}^2\exp(\lambda t) = 0$, leading to the characteristic equation

$$\lambda^2 + 2\zeta\omega_n\lambda + \omega_n^2 = 0. \tag{7.4}$$

Solving for the roots yields $\lambda_{1,2} = \omega_n(-\zeta \pm \sqrt{\zeta^2 - 1})$. The general solution is $r = A_1\exp(\lambda_1 t) + A_2\exp(\lambda_2 t)$. Depending on the value of ζ, the solution will have one of three distinct types of behavior:

- $\zeta > 1$, overdamped, leading to no oscillation, where the value of r approaches zero for large values of time. Mathematically, λ_1 and λ_2 are negative numbers, thus $r_{\mathrm{H}} = A_1\exp(\omega_{\mathrm{n}}(-\zeta + \sqrt{\zeta^2-1})t) + A_2\exp(\omega_{\mathrm{n}}(-\zeta - \sqrt{\zeta^2-1})t)$.
- $\zeta = 1$, critically damped, leading to no oscillation, where the value of r approaches zero for large values of time, however faster than the overdamped solution. Mathematically, λ_1 and λ_2 are equal real numbers, $\lambda_1 = \lambda_2 = -\omega_n$, thus $r_{\mathrm{H}} = (A_1 + A_2 t)\exp(\omega_{\mathrm{n}} t)$.
- $\zeta < 1$, underdamped, leading to damped oscillation, where the value of r approaches zero for large values of time, in an oscillatory fashion. Mathematically, $\zeta^2 - 1 < 0$, thus $r_{\mathrm{H}} = A_1\cos(\omega_{\mathrm{d}} t) + A_2\sin(\omega_{\mathrm{d}} t)$.

Thus, under certain conditions, a granular flow can vibrate. The particular solution, generated by the presence of externally applied forces, which satisfies the differential equation for a specific right-hand side

[15] Typically, the simulations took under a minute on a single high performance laptop.

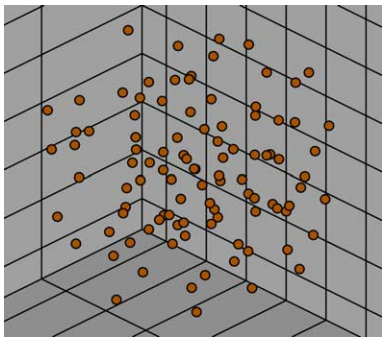

Fig. 4. The starting configuration for the granular flow.

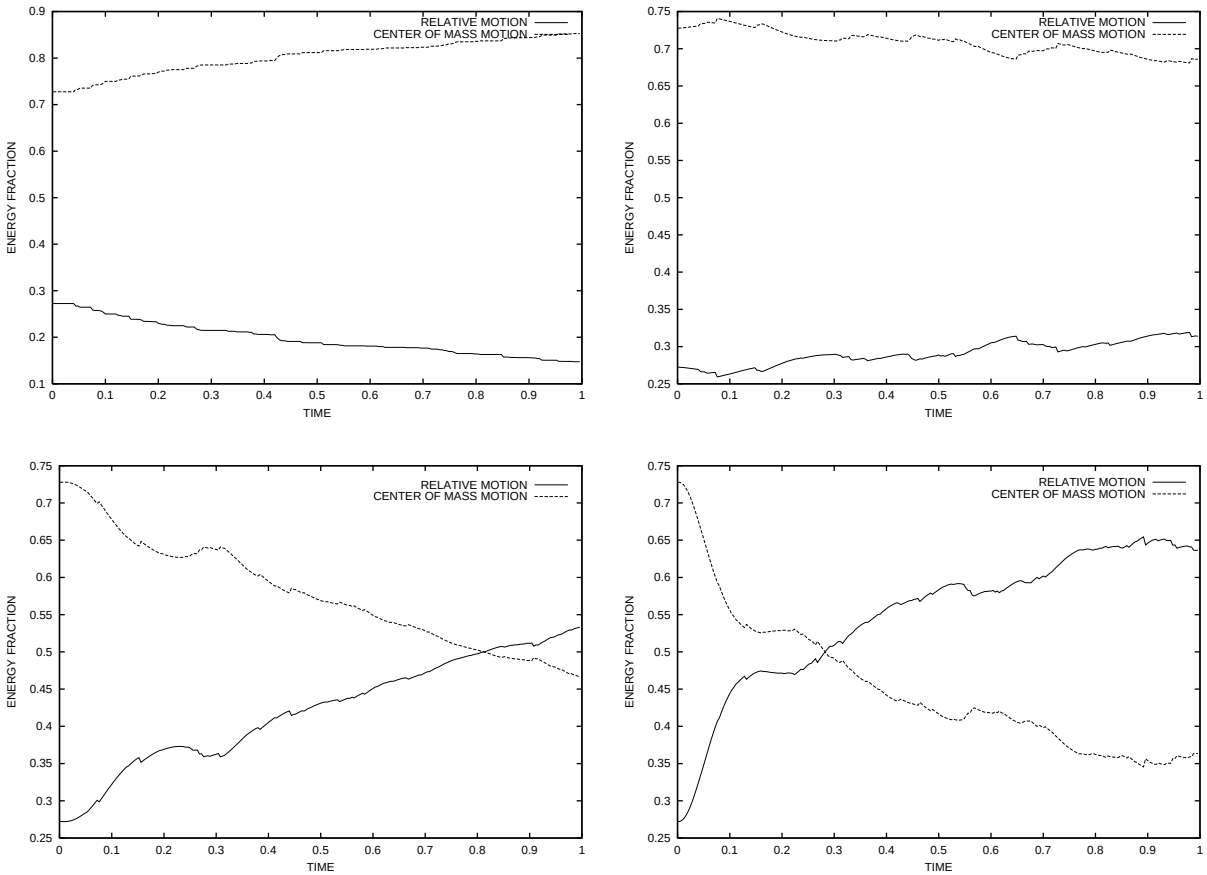

Fig. 5. The proportions of the kinetic energy that are bulk and relative motion. Starting from left to right and top to bottom, with $e_0 = 0.5$, $\mu_s = 0.2$, $\mu_d = 0.1$: (1) no near-field interaction, (2) $\overline{\alpha}_1 = 0.1$ and $\overline{\alpha}_2 = 0.05$, (3) $\overline{\alpha}_1 = 0.25$ and $\overline{\alpha}_2 = 0.125$ and (4) $\overline{\alpha}_1 = 0.5$ and $\overline{\alpha}_2 = 0.25$.

$$\ddot{r}_P + 2\zeta\omega_n\dot{r}_P + \omega_n^2 r_P = \frac{f(t)}{m}, \tag{7.5}$$

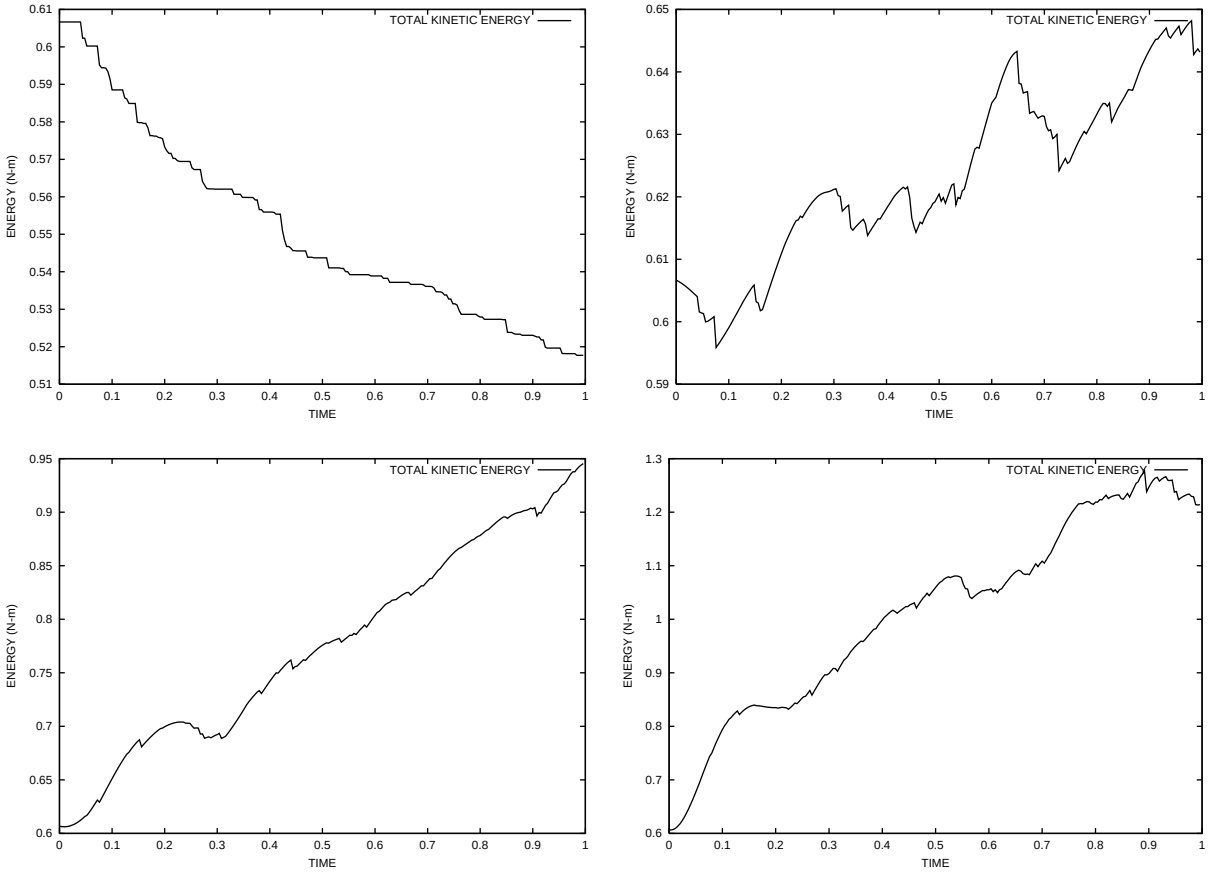

Fig. 6. The total kinetic energy in the system per unit mass. Starting from left to right and top to bottom, with $e_0 = 0.5$, $\mu_s = 0.2$, $\mu_d = 0.1$: (1) no near-field interaction, (2) $\overline{\alpha}_1 = 0.1$ and $\overline{\alpha}_2 = 0.05$, (3) $\overline{\alpha}_1 = 0.25$ and $\overline{\alpha}_2 = 0.125$ and (4) $\overline{\alpha}_1 = 0.5$ and $\overline{\alpha}_2 = 0.25$.

For example if $f(t) = f_0 \sin(\Omega t)$,

$$r_P = R \sin(\Omega t - \phi), \tag{7.6}$$

where

$$R = \frac{f_0}{k\sqrt{\left(1 - \frac{\Omega^2}{\omega_n^2}\right)^2 + \left(2\zeta \frac{\Omega}{\omega_n}\right)^2}} \tag{7.7}$$

and

$$\phi = \tan^{-1}\left(\frac{2\zeta \frac{\Omega}{\omega_n}}{1 - \frac{\Omega^2}{\omega_n^2}}\right). \tag{7.8}$$

Thus, clearly, such granular systems may resonate if forced at certain frequencies. In order to qualitatively tie this directly to the form of problem considered in this work, consider a linearization of a single nonlinear differential equation, describing the attraction and repulsion from the origin ($r_0 = 0$) of the form [16]

$$m\ddot{r} + d\dot{r} = \Psi^{\mathrm{nf}}(r), \tag{7.9}$$

where $\Psi^{\mathrm{nf}}(r) = -\alpha_1 r^{-\beta_1} + \alpha_2 r^{-\beta_2}$ and where d is an effective dissipation term, which would arise from inelastic impact and friction. Upon linearization of the non-linear interaction relation about a point r_*, $\Psi^{\mathrm{nf}}(r) \approx \Psi^{\mathrm{nf}}(r_*) + \frac{\partial \Psi^{\mathrm{nf}}}{\partial r}|_{r=r_*}(r - r_*) + \mathcal{O}(r - r_*)$, and normalizing the equations, we obtain

$$\ddot{r} + 2\zeta^* \omega_{\mathrm{n}}^* \dot{r} + (\omega_{\mathrm{n}}^*)^2 r = \frac{f^*(t)}{m}, \tag{7.10}$$

where $\omega_n^* = \sqrt{\frac{-\frac{\partial \Psi^{\mathrm{nf}}}{\partial r}|_{r=r_*}}{m}}$, where $\zeta^* = \frac{d}{2m\omega_n^*}$ and where $f^*(t) = \Psi^{\mathrm{nf}}(r_*) - \frac{\partial \Psi^{\mathrm{nf}}}{\partial r}|_{r=r_*} r_*$. For the specific interaction form chosen we have

$$\omega_n^* = \sqrt{\frac{-\alpha_1\beta_1 r_*^{-\beta_1-1} + \alpha_2\beta_2 r_*^{-\beta_2-1}}{m}} = \sqrt{-\overline{\alpha}_1 m\beta_1 r_*^{-\beta_1-1} + \overline{\alpha}_2 m\beta_2 r_*^{-\beta_2-1}}, \tag{7.11}$$

and where the "loading" is

$$f^*(t) = -\alpha_1 r_*^{-\beta_1} + \alpha_2 r_*^{-\beta_2} - \alpha_1\beta_1 r_*^{-\beta_1-1} + \alpha_2\beta_2 r_*^{-\beta_2-1}. \tag{7.12}$$

We note that if the following special choice of parameters, as in the preceding simulations, is made, $(\beta_1, \beta_2) = (1, 2)$, and r_* is chosen as the static equilibrium point, r_{e}, given by Eq. (2.7), then $r_* = r_{\mathrm{e}} = \frac{\alpha_2}{\alpha_1}$, and

$$\omega_{\mathrm{n}}^* = \sqrt{\frac{\alpha_1\left(\frac{\alpha_1}{\alpha_2}\right)^2}{m}} = \sqrt{\frac{\alpha_1}{m}\left(\frac{\overline{\alpha}_1}{\overline{\alpha}_2}\right)^2} \stackrel{\mathrm{def}}{=} \sqrt{\frac{k^*}{m}}, \tag{7.13}$$

where $k^* \stackrel{\mathrm{def}}{=} \alpha_1\left(\frac{\overline{\alpha}_1}{\overline{\alpha}_2}\right)^2$. Thus, in the preceding examples, when we had kept the ratio $\frac{\overline{\alpha}_1}{\overline{\alpha}_2}$ constant, however increasing α_1 (while keeping m constant), we were effectively increasing the "stiffness" in the system and the amount of (pre-)stored energy available to counteract dissipation. Clearly, under certain conditions, a granular flow may "pulse" (oscillate) or decay depending on the character of the interaction and the contact parameters. Thus, non-monotone behavior is not unexpected for the multibody system (Fig. 6). We remark that, increasingly smaller ω_{n}^* indicates that the system tends toward a "regular" (near-field free) granular flow. Smaller ω_{n}^* would occur with heavier particles or smaller attractive forces, and larger values of ζ^* (more damped) will occur when increased friction or smaller restitution coefficients are present in the flow. Clearly, key dimensionless parameters, like ζ^*, which characterize the oscillatory behavior, and thus relative, fluctuating, motion with respect to the mean, within the the granular flow.

8. Inverse problems/parameter identification

An important aspect of any model is the inverse problem of identification of parameters which force the system behavior to match a target response. In the ideal case, one would like to determine the type of near-field interaction that produces certain granular flow characteristics, via numerical simulations, in order to minimize time-consuming laboratory tests. As a representative of a class of model problems, consider inverse problems whereby the parameters in the near-field interaction representation are sought, the α's and β's, which deliver a target granular flow behavior by minimizing a normalized cost function

[16] The unit normal has been taken into account, thus the presence of a change in sign.

$$\Pi = \frac{\left(\int_0^{\mathscr{T}} \mid A - A^* \mid \mathrm{d}t\right)}{\int_0^{\mathscr{T}} \mid A^* \mid \mathrm{d}t}, \tag{8.1}$$

where total simulation time is $\mathscr{T}$, where A is a computationally generated quantity of interest and where A^* is the target response. Typically, for the class of problems considered in this work, formulations such as in Eq. (8.1) depend in a non-convex and non-differentiable manner, on the α's and β's. This is primarily due to the physics of sudden intergranular impact and transient dynamics. Clearly, we have restrictions on the parameters in the near-field interaction $\alpha^-_{1\,\mathrm{or}\,2} \leqslant \alpha_{1\,\mathrm{or}\,2} \leqslant \alpha^+_{1\,\mathrm{or}\,2}$ and $\beta^-_{1\,\mathrm{or}\,2} \leqslant \beta_{1\,\mathrm{or}\,2} \leqslant \beta^+_{1\,\mathrm{or}\,2}$, where $\alpha^-_{1\,\mathrm{or}\,2}$, $\alpha^+_{1\,\mathrm{or}\,2}$, $\beta^-_{1\,\mathrm{or}\,2}$ and $\beta^+_{1\,\mathrm{or}\,2}$ are the lower and upper limits coefficients in the interaction forces. [17] With respect to the minimization of Eq. (8.1), classical gradient-based deterministic optimization techniques are not robust, due to difficulties with objective function non-convexity and non-differentiability. Classical gradient-based algorithms are likely to converge only toward a local minimum of the objective functional if an accurate initial guess to the global minimum is not provided. Also, usually it is extremely difficult to construct an initial guess that lies within the (global) convergence radius of a gradient-based method. These difficulties can be circumvented by the use of a certain class of non-derivative search methods, usually termed "genetic" algorithms (GA), before applying gradient-based schemes. Genetic algorithms are search methods based on the principles of natural selection, employing concepts of species evolution, such as reproduction, mutation and crossover. Implementation typically involves a randomly generated population of fixed-length elemental strings, "genetic information", each of which represents a specific choice of system parameters. The population of individuals undergo "mating sequences" and other biologically-inspired events in order to find promising regions of the search space. There are a variety of such methods, which employ concepts of species evolution, such as reproduction, mutation and crossover. Such methods primarily stem from the work of John Holland (Holland, 1975). For reviews of such methods, see, for example, Goldberg (1989), Davis (1991), Onwubiko (2000),Kennedy and Eberhart (2001) and Goldberg and Deb (2000).

8.1. A genetic algorithm

As examples of objective functions that one might minimize, consider:

- Overall energetic behavior per unit mass:

$$\Pi_{\mathrm{E}} = \frac{\int_0^{\mathscr{T}} \mid \overline{T} - \overline{T}^* \mid \mathrm{d}t}{\int_0^{\mathscr{T}} \overline{T}^* \mathrm{d}t}, \tag{8.2}$$

  where total simulation time is $\mathscr{T}$ and where $\overline{T}^*$ is a target value.
- Energy component distribution, for the relative motion part

$$\Pi_{\mathrm{Er}} = \frac{\int_0^{\mathscr{T}} \mid T_{\mathrm{r}} - T^*_{\mathrm{r}} \mid \mathrm{d}t}{\int_0^{\mathscr{T}} T^*_{\mathrm{r}} \mathrm{d}t}, \tag{8.3}$$

  and for the bulk motion part

$$\Pi_{\mathrm{Eb}} = \frac{\int_0^{\mathscr{T}} \mid T_{\mathrm{b}} - T^*_{\mathrm{b}} \mid \mathrm{d}t}{\int_0^{\mathscr{T}} T^*_{\mathrm{b}} \mathrm{d}t}, \tag{8.4}$$

where the fraction of kinetic energy due to relative motion is T_{r}, where the fraction of kinetic energy due to bulk motion is T_{b}, and where T^*_{r} and T^*_{b} are the target values.

[17] Additionally, we could also vary the other parameters in the system, such as the friction, particle densities, drag, etc. However, we shall fix these parameters during the upcoming examples.

Compactly, one may write

$$\Pi = \frac{w_{\mathrm{E}}\Pi_{\mathrm{E}} + w_{\mathrm{Er}}\Pi_{\mathrm{Er}} + w_{\mathrm{Eb}}\Pi_{\mathrm{Eb}}}{w_{\mathrm{E}} + w_{\mathrm{Er}} + w_{\mathrm{Eb}}}. \tag{8.5}$$

Adopting the approaches found in Zohdi Zohdi (2003a,b,c, in press), a genetic algorithm has been developed to treat non-convex inverse problems involving various aspects of multi-particle mechanics. The central idea is that the system parameters form a genetic string and a survival of the fittest algorithm is applied to a population of such strings. The overall process is (a) a population (S) of different parameter sets are generated at random within the parameter space, each represented by a (''genetic'') string of the system (N) parameters, (b) the performance of each parameter set is tested, (c) the parameter sets are ranked from top to bottom according to their performance, (d) the best parameter sets (parents) are mated pairwise producing two offspring (children), i.e. each best pair exchanges information by taking random convex combinations of the parameter set components of the parents' genetic strings and (e) the worst performing genetic strings are eliminated, new replacement parameter sets (genetic strings) are introduced into the remaining population of best performing genetic strings and the process (a–e) is then repeated. The term ''fitness'' of a genetic string is used to indicate the value of the objective function. The most fit genetic string is the one with the smallest objective function. The retention of the top fit genetic strings from a previous generation (parents) is critical, since if the objective functions are highly non-convex (the present case), there exists a clear possibility that the inferior offspring will replace superior parents. When the top parents are retained, the minimization of the cost function is guaranteed to be monotone (guaranteed improvement) with increasing generations. There is no guarantee of successive improvement if the top parents are not retained, even though non-retention of parents allows more new genetic strings to be evaluated in the next generation. Numerical studies conducted by the author imply that, for sufficiently large populations, the benefits of parent retention outweigh this advantage and any disadvantages of ''inbreeding'', i.e. a stagnant population. For more details on this so-called ''inheritance property'' see Davis (1991) or Kennedy and Eberhart (2001). In the upcoming algorithm, inbreeding is mitigated since, with each new generation, new parameter sets, selected at random within the parameter space, are added to the population. Previous numerical studies of the author (Zohdi, 2003c) have indicated that not retaining the parents is suboptimal due to the possibility that inferior offspring will replace superior parents. Additionally, parent retention is computationally less expensive, since these parameter sets do not have to be reevaluated in the next generation.

An implementation of such ideas is as follows (Zohdi, 2003a,b,c, in press):

- *Step 1:* Randomly generate a population of S starting genetic strings, $\boldsymbol{\Lambda}^i$ $(i = 1, \ldots, S)$: $\boldsymbol{\Lambda}^i \stackrel{\mathrm{def}}{=} \{\Lambda_1^i, \Lambda_2^i, \Lambda_3^i, \Lambda_4^i, \ldots, \Lambda_N^i\} = \{\overline{\alpha}_1^i, \beta_1^i, \overline{\alpha}_2^i, \beta_2^i, \ldots\}$.
- *Step 2:* Compute fitness of each string $\Pi(\boldsymbol{\Lambda}^i)$ $(i = 1, \ldots, S)$.
- *Step 3:* Rank genetic strings: $\boldsymbol{\Lambda}^i (i = 1, \ldots, S)$.
- *Step 4:* Mate nearest pairs and produce two offspring $(i = 1, \ldots, S)$. $\boldsymbol{\lambda}^i \stackrel{\mathrm{def}}{=} \Phi^{(\mathrm{I})}\boldsymbol{\Lambda}^i + (1 - \Phi^{(\mathrm{I})})\boldsymbol{\Lambda}^{i+1}$, $\boldsymbol{\lambda}^{i+1} \stackrel{\mathrm{def}}{=} \Phi^{(\mathrm{II})}\boldsymbol{\Lambda}^i + (1 - \Phi^{(\mathrm{II})})\boldsymbol{\Lambda}^{i+1}$
- *Note:* $\Phi^{(\mathrm{I})}$ and $\Phi^{(\mathrm{II})}$ are random numbers, such that $0 \leqslant \Phi^{(\mathrm{I})}, \Phi^{(\mathrm{II})} \leqslant 1$, which are different for each component of each genetic string.
- *Step 5:* Kill off bottom $M < S$ strings and keep top $K < N$ parents and top K offspring (Koffspring + K parents + $M = S$).
- *Step 6:* Repeat STEPS 1–6 with top gene pool (K offspring and K parents), plus M new, randomly generated, strings.
- *Option:* Rescale and restart search around best performing parameter set every few generations.

- *Option:* We remark that gradient-based methods are sometimes useful for post-processing solutions found with a genetic algorithm, if the objective function is sufficiently smooth in that region of the parameter space. In other words, if one has located convex portion of the parameter space with a global genetic search, one can employ gradient-based procedures locally to minimize the objective function further. In such procedures, in order to obtain a new directional step for $\mathbf{\Lambda}$, one must solve the following system, $[\mathbb{H}]\{\Delta\mathbf{\Lambda}\} = -\{\boldsymbol{g}\}$, where $[\mathbb{H}]$ is the Hessian matrix ($N \times N$), where $\{\Delta\mathbf{\Lambda}\}$ is the parameter increment ($N \times 1$), and $\{\boldsymbol{g}\}$ is the gradient ($N \times 1$). We shall not employ this second (post-genetic) stage in this work. An exhaustive review of these methods can be found in the well-known texts of Luenberger (1974) or Gill et al. (1995).

Remarks. It is important to scale the system variables, for example, to be positive numbers and of comparable magnitude, in order to avoid dealing with large variations in the parameter vector components. Typically, for granular flows with a finite number of particles, there will be slight variations in the performance for different random starting configurations. In order to stabilize the objective function's value with respect to the randomness of the flow starting configuration, for a given parameter selection ($\mathbf{\Lambda}$, characterized by the α's and β's), a regularization procedure is applied within the genetic algorithm, whereby the performances of a series of different random starting configurations are averaged until the (ensemble) average converges, i.e. until the following condition is met: $\left|\frac{1}{E+1}\sum_{i=1}^{E+1} \Pi^{(i)}(\mathbf{\Lambda}^{\mathrm{I}}) - \frac{1}{E}\sum_{i=1}^{E} \Pi^{(i)}(\mathbf{\Lambda}^{\mathrm{I}})\right| \leqslant \mathrm{TOL}\left|\frac{1}{E+1}\sum_{i=1}^{E+1} \Pi^{(i)}(\mathbf{\Lambda}^{\mathrm{I}})\right|$, where index i indicates a different starting random configuration ($i = 1, 2, \ldots, E$) that has been generated and E indicates the total number of configurations tested. In order to implement this in the genetic algorithm, in STEP 2, one simply replaces *compute* with *ensemble compute*, which requires a further inner loop to test the performance of multiple starting configurations. Similar ideas have been applied to randomly dispersed particulate media in Zohdi (2003a,b,c, in press).

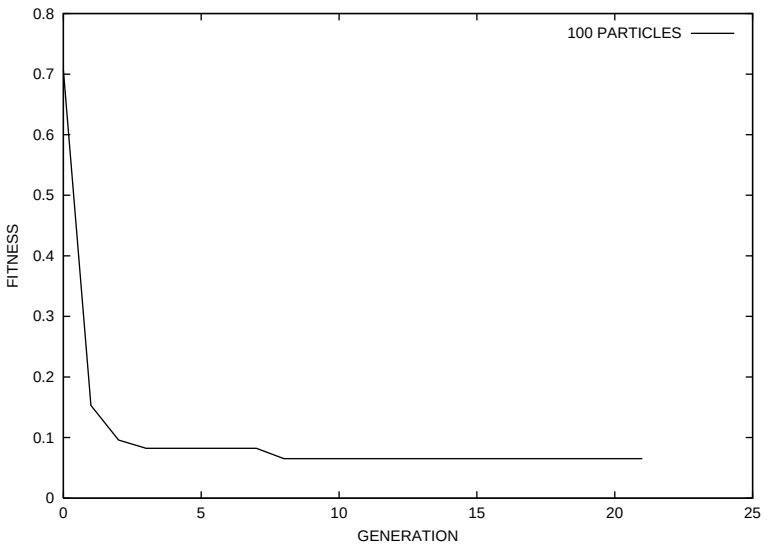

Fig. 7. The best parameter set's ($\overline{\alpha}_1$, $\overline{\alpha}_2, \beta_1, \beta_2$) objective function value with passing generations.

Table 1
The optimal coefficients of attraction and repulsion for the granular flow and the top six fitnesses

Rank	$\overline{\alpha}_1$	β_1	$\overline{\alpha}_2$	β_2	Π
1	0.35935	0.67398	0.25659	1.58766	0.065228
2	0.31214	0.67816	0.22113	1.65054	0.065690
3	0.30032	0.54474	0.22240	1.51649	0.070433
4	0.31143	0.57278	0.25503	1.36696	0.073200
5	0.32872	0.74653	0.25560	1.56315	0.078229
6	0.30580	0.74276	0.27228	1.36962	0.090701

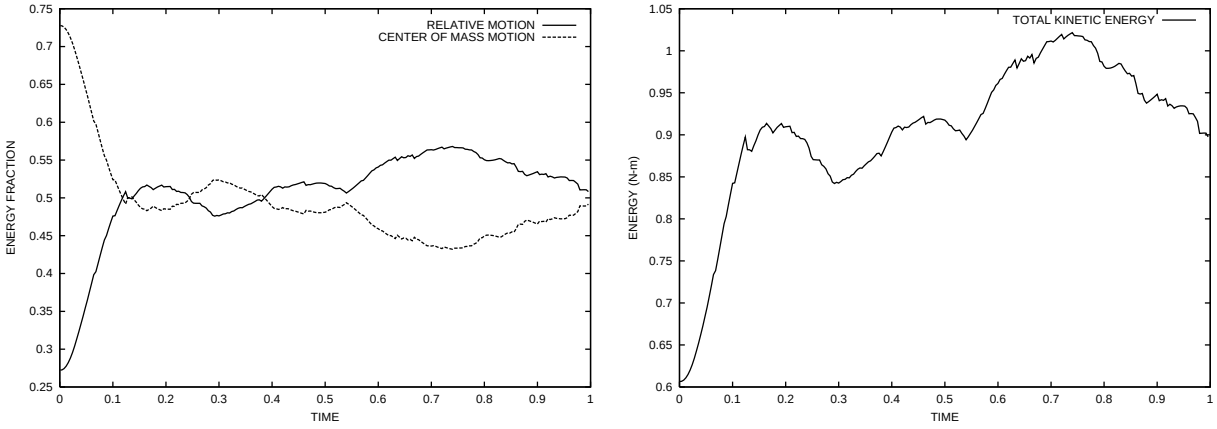

Fig. 8. Simulation results using the best parameter set's ($\overline{\alpha}_1$, $\overline{\alpha}_2, \beta_1, \beta_2$) values (for one random realization).

8.2. A numerical example

We considered a search space of $0 \leqslant \overline{\alpha}_1 \leqslant 1$, $0 \leqslant \beta_1 \leqslant 1$, $0 \leqslant \overline{\alpha}_2 \leqslant 1$ and $1 \leqslant \beta_2 \leqslant 2$. Recall the stability restriction on the exponents were $\frac{\beta_2}{\beta_1} > 1$, thus the choice of the range of search. As in the previous simulations, 100 particles, with periodic boundary conditions were used. The total time was set to be one second ($\mathscr{T} = 1$). The starting state values of the system were the same as in the previous examples. The target objective (behavior) values where constants: $(\overline{T}^*, T_b^*, T_r^*) = (1.0, 0.5, 0.5)$. Such an objective can be interpreted as forcing a system with given initial behavior to adapt to a different type of behavior within a given time interval. The number of genetic strings in the population was set to 20, for 20 generations, allowing six offspring of the top six parents, along with their parents, to proceed to the next generation. Therefore, after each generation, eight entirely new genetic strings are introduced. Every 10 generations, the search was re-scaled around the best parameter set, and the search restarted. Fig. 7 and Table 1 depict the results. A total of 310 parameter selections were tested. The total number of strings tested was 1757, thus requiring an average of 5.68 strings per parameter selection for the ensemble averaging stabilization. The behavior of the best parameter selection's response is shown in Fig. 8.

9. Concluding remarks

In the this work, a general model was developed for the impact of charged granular media. The specific structure of the interaction forces chosen was only one of many possibilities to model NF-granular flow

behavior. Other potentials, to produce the interaction forces, for example, from the field of molecular dynamics (MD), are possible. For an extensive survey of MD-type interaction forces, which includes comparisons of the theoretical and computational properties of each interaction law, we refer the reader to Frenklach and Carmer (1999). The analogy between granular flow dynamics and molecular dynamics (MD) of an atomistic chemical system is inescapable. In the usual MD approach (see Haile, 1992, for example), the motion of individual atoms is described by the Newton's Second Law with the forces computed from a prescribed potential energy function, $V(\boldsymbol{r})$, $m\ddot{\boldsymbol{r}} = -\nabla V(\boldsymbol{r})$. The MD approach has been applied to description of all material phases: solids, liquids, and gases, as well as biological systems (Hase, 1999; Schlick, 2000). For instance, a Fourier transform of the velocity autocorrelation function specifies "bulk" diffusion coefficient (Rapaport, 1995). The mathematical form of more sophisticated potentials to produce interaction forces, $\boldsymbol{\Psi}^{\mathrm{nf}} = -\nabla V$, are rooted in the expansion,

$$V = \sum_{i,j} V_2 + \sum_{i,j,k} V_3 + \cdots, \tag{9.1}$$

where V_2 is the binary, V_3 tertiary, etc., potential energy functions, and the summations are taken over corresponding combinations of atoms. The binary functions usually take the form of the familiar Mie, Lennard-Jones, and Morse potentials (Moelwyn-Hughes, 1961). The expansions beyond the binary interactions introduce either three-body terms directly (Stillinger and Weber, 1985) or as "local" modifications of the two-body terms (Tersoff, 1988). Clearly, the inverse parameter identification technique presented is applicable to such representations, however with more adjustable search parameters. For examples with significantly more search parameter complexity, see Zohdi (2003a,b,c, in press).

Appendix A. Properties of a potential

A force field $\boldsymbol{\Psi}^{\mathrm{nf}}$ is said to be conservative if and only if there exists a continuously differentiable scalar field V such that $\boldsymbol{\Psi}^{\mathrm{nf}} = -\nabla V$. If the force field is conservative, with potential V, then a necessary and sufficient condition for a particle to be in equilibrium at that point is that

$$\boldsymbol{\Psi}^{\mathrm{nf}} = -\nabla V = \boldsymbol{0}, \tag{A.1}$$

in other words $\frac{\partial V}{\partial x_1} = 0$, $\frac{\partial V}{\partial x_2} = 0$ and $\frac{\partial V}{\partial x_3} = 0$. Forces acting on a particle that are (1) always directed toward or away another point and (2) whose magnitude depend only on the distance between the particle and the point of attraction/repulsion are called *central forces*. They have the form

$$\boldsymbol{\Psi}^{\mathrm{nf}} = -\mathscr{C}(\|\boldsymbol{r} - \boldsymbol{r}_0\|)\frac{\boldsymbol{r} - \boldsymbol{r}_0}{\|\boldsymbol{r} - \boldsymbol{r}_0\|} = \mathscr{C}(\|\boldsymbol{r} - \boldsymbol{r}_0\|)\boldsymbol{n}, \tag{A.2}$$

where $\boldsymbol{r}$ is the position of the particle, where $\boldsymbol{r}_0$ is the position of a point of attraction/repulsion and where $\boldsymbol{n} = \frac{\boldsymbol{r}_0 - \boldsymbol{r}}{\|\boldsymbol{r} - \boldsymbol{r}_0\|}$. The central force is one of attraction if $\mathscr{C}(\|\boldsymbol{r} - \boldsymbol{r}_0\|) > 0$ and one of repulsion if $\mathscr{C}(\|\boldsymbol{r} - \boldsymbol{r}_0\|) < 0$. We remark that a central force field is always conservative, since $\nabla \times \boldsymbol{\Psi}^{\mathrm{nf}} = \boldsymbol{0}$. For example, consider

$$V = \underbrace{\frac{\alpha_1\|\boldsymbol{r} - \boldsymbol{r}_0\|^{-\beta_1+1}}{-\beta_1 + 1}}_{\text{attraction}} - \underbrace{\frac{\alpha_2\|\boldsymbol{r} - \boldsymbol{r}_0\|^{-\beta_2+1}}{-\beta_2 + 1}}_{\text{repulsion}}, \tag{A.3}$$

where all of the parameters, α's and β's, are non-negative. The gradient yields

$$-\nabla V = \boldsymbol{\Psi}^{\mathrm{nf}} = (\alpha_1\|\boldsymbol{r} - \boldsymbol{r}_0\|^{-\beta_1} - \alpha_2\|\boldsymbol{r} - \boldsymbol{r}_0\|^{-\beta_2})\boldsymbol{n}, \tag{A.4}$$

which is the form used in the text. If a particle which is displaced slightly from an equilibrium point tends to return to that point, then we call that point a point of stability or stable point and the equilibrium is said to

be stable. Otherwise we say that the point is one of instability and the equilibrium is unstable. *A necessary and sufficient condition that an equilibrium point be one of stability is that the potential V at the point be a minimum.* The general condition by which a potential is stable for the multidimensional case can be determined by studying the properties of the Hessian,

$$[\mathbb{H}] \stackrel{\text{def}}{=} \begin{bmatrix} \frac{\partial^2 V}{\partial x_1 \partial x_1} & \frac{\partial^2 V}{\partial x_1 \partial x_2} & \frac{\partial^2 V}{\partial x_1 \partial x_3} \\ \frac{\partial^2 V}{\partial x_2 \partial x_1} & \frac{\partial^2 V}{\partial x_2 \partial x_2} & \frac{\partial^2 V}{\partial x_2 \partial x_3} \\ \frac{\partial^2 V}{\partial x_3 \partial x_1} & \frac{\partial^2 V}{\partial x_3 \partial x_2} & \frac{\partial^2 V}{\partial x_3 \partial x_3} \end{bmatrix}, \tag{A.5}$$

around an equilibrium point. A sufficient condition for V to attain a minimum at an equilibrium point is that the Hessian be positive definite (which implies that V is locally convex). For more details see Hale and Kocak (1991).

Remark. Clearly, the central force potential chosen in this work is stable for motion in the normal direction, i.e. the line connecting the centers of the particles. For disturbances in directions orthogonal to the normal direction, the potential is neutrally stable, i.e. the Hessian's determinant is zero, thus indicating that the potential does not change for such perturbations.

References

Axelsson, O., 1994. Iterative Solution Methods. Cambridge University Press.

Behringer, R.P., 1993. The dynamics of flowing sand. Nonlinear Sci. Today 3, 1.

Behringer, R.P., Baxter, G.W., 1993. Pattern Formation, Complexity & Time-Dependence. In: Mehta, A. (Ed.), Granular Flows. Granular Matter—An Interdisciplinary Approach. Springer-Verlag, New York, pp. 85–119.

Behringer, R.P., Miller, B.J., 1997. Stress Fluctuations For Sheared 3D Granular Materials. In: Behringer, R., Jenkins, J. (Eds.), Proceedings, Powders & Grains 97. Balkema, pp. 333–336.

Behringer, R.P., Howell, D., Veje, C., 1999. Fluctuations in granular flows. Chaos 9, 559–572.

Berezin, Y.A., Hutter, K., Spodareva, L.A., 1998. Stability properties of shallow granular flows. Int. J. NonLinear Mech. 33 (4), 647–658.

Cho, H., Barber, J.R., 1999. Stability of the three-dimensional Coloumb friction law. Proc. Roy. Soc. 455 (1983), 839–862.

Davis, L., 1991. Handbook of Genetic Algorithms. Thompson Computer Press.

St. Doltsinis, I., 1993. Coupled field problems–solution techniques for sequential & parallel processing. In: Papadrakakis, M. (Ed.), Solving large-scale problems in mechanics.

St. Doltsinis, I., 1997. Solution of coupled systems by distinct operators. Eng. Comput. 14, 829–868.

Frenklach, M., Carmer, C.S., 1999. Molecular dynamics using combined quantum & empirical forces: application to surface reactions. Advances in Classical Trajectory Methods, vol. 4. JAI Press.

Gill, P., Murray, W., Wright, M., 1995. Practical Optimization. Academic Press.

Goldberg, D.E., 1989. Genetic Algorithms in Search, Optimization & Machine Learning. Addison-Wesley.

Goldberg, D.E., Deb, K., 2000. Special issue on Genetic Algorithms. Comput. Meth. Appl. Mech. Eng. 186 (2–4), 121–124.

Goldsmith, W., 2001. Impact: The Theory & Physical Behavior of Colliding Solids. Dover Re-issue, Toronto.

Gray, J.M.N.T., Wieland, M., Hutter, K., 1999. Gravity-driven free surface flow of granular avalanches over complex basal topography. Proc. Roy. Soc. Lond. A 455, 1841–1874.

Gray, J.M.N.T., Hutter, K., 1997. Pattern formation in granular avalanches. Continuum Mech. Thermodynam. 9, 341–345.

Gray, J.M.N.T., 2001. Granular flow in partially filled slowly rotating drums. J. Fluid Mech. 441, 1–29.

Greve, R., Hutter, K., 1993. Motion of a granular avalanche in a convex & concave curved chute: experiments & theoretical predictions. Philos. Trans. Roy. Soc. Lond. A 342, 573–600.

Haile, J.M., 1992. Molecular Dynamics Simulations: Elementary Methods. Wiley.

Hale, J., Kocak, H., 1991. Dynamics & Bifurcations. Springer-Verlag.

Hase, W.L., 1999. Molecular Dynamics of Clusters, Surfaces, Liquids, & InterfacesAdvances in Classical Trajectory Methods, vol. 4. JAI Press.

Holland, J.H., 1975. Adaptation in Natural & Artificial Systems. University of Michigan Press, Ann Arbor, MI.

Hutter, K., 1996. Avalanche dynamics. In: Singh, V.P. (Ed.), Hydrology of Disasters. Kluwer Academic Publishers, Dordrecht, pp. 317–394.
Hutter, K., Koch, T., Plüss, C., Savage, S.B., 1995. The dynamics of avalanches of granular materials from initiation to runout. Part II. Experiments. Acta Mech. 109, 127–165.
Hutter, K., Rajagopal, K.R., 1994. On flows of granular materials. Continuum Mech. Thermodynam. 6, 81–139.
Hutter, K., Siegel, M., Savage, S.B., Nohguchi, Y., 1993. Two-dimensional spreading of a granular avalanche down an inclined plane. Part I: Theory. Acta Mech. 100, 37–68.
Jaeger, H.M., Nagel, S.R., 1992a. La Physique de l'Etat Granulaire. La Recherche 249, 1380.
Jaeger, H.M., Nagel, S.R., 1992b. Physics of the granular state. Science 255, 1523.
Jaeger, H.M., Nagel, S.R., 1993. La Fisica del Estado Granular. Mundo Cientifico 132, 108.
Jaeger, H.M., Knight, J.B., Liu, C.-h., Nagel, S.R., 1994. What is shaking in the sand box? Mater. Res. Soc. Bull. 19, 25.
Jaeger, H.M., Nagel, S.R., Behringer, R.P., 1996a. The physics of granular materials. Phys. Today 4, 32.
Jaeger, H.M., Nagel, S.R., Behringer, R.P., 1996b. Granular solids, liquids & gases. Rev. Mod. Phys. 68, 1259.
Jaeger, H.M., Nagel, S.R., 1997. Dynamics of Granular Material. Am. Sci. 85, 540.
Johnson, K., 1985. Contact Mechanics. Cambridge University Press.
Kennedy, J., Eberhart, R., 2001. Swarm Intelligence. Morgan Kaufmann Publishers.
Kikuchi, N., Oden, J.T., 1988. Contact Problems in Elasticity: A Study of Variational Inequalities & Finite Element Methods. SIAM, Philadelphia, PA.
Klarbring, A., 1990. Examples of nonuniqueness & nonexistence of solutions to quasistatic contact problems with friction. Ingenieur-Archiv 60, 529–541.
Koch, T., Greve, R., Hutter, K., 1994. Unconfined flow of granular avalanches along a partly curved surface. II. Experiments & numerical computations. Proc. Roy. Soc. Lond. A 445, 415–435.
Le Tallec, P., Mouro, J., 2001. Fluid structure interaction with large structural displacements. Comp. Meth. Appl. Mech. Eng. 190 (24–25), 3039–3067.
Lewis, R.W., Schrefler, B.A., 1998. The Finite Element Method in the Static & Dynamic Deformation & Consolidation of Porous Media, 2nd ed. Wiley Press.
Lewis, R.W., Schrefler, B.A., Simoni, L., 1992. Coupling versus uncoupling in soil consolidation. Int. J. Num. Anal. Meth. Geomech. 15, 533–548.
Liu, C.-h., Jaeger, H.M., Nagel, S.R., 1991. Finite size effects in a sandpile. Phys. Rev. A 43, 7091.
Liu, C.-h., Nagel, S.R., 1993. Sound in a granular material: disorder & nonlinearity. Phys. Rev. B 48, 15646.
Luenberger, D., 1974. Introduction to Linear & Nonlinear Programming. Addison-Wesley, Menlo Park.
Martins, J.A.C., Oden, J.T., 1987. Existence & uniqueness results in dynamics contact problems with nonlinear normal & friction interfaces. Nonlinear Anal. 11, 407–428.
Meyers, M.A., 1994. Dynamic Behavior of Materials. Wiley.
Moelwyn-Hughes, E.A., 1961. Physical Chemistry. Pergamon Press.
Nagel, S.R., 1992. Instabilities in a sandpile. Rev. Mod. Phys. 64, 321.
Nesterenko, V.F., Meyers, M.A., Chen, H.C., LaSalvia, J.C., 1994. Controlled high rate localized shear in porous reactive media. Appl. Phys. Lett. 65 (24), 3069–3071.
Nesterenko, V.F., 2001. Dynamics of Heterogeneous Materials. Springer-Verlag.
Oden, J.T., Pires, E., 1983. Nonlocal & nonlinear friction laws & variational principles for contact problems in elasticity. ASME J. Appl. Mech. 50, 67–76.
Onwubiko, C., 2000. Introduction to Engineering Design Optimization. Prentice-Hall.
Park, K.C., Felippa, C.A., 1983. Partitioned analysis of coupled systems. In: Belytschko, T., Hughes, T.J.R. (Eds.), Computational Methods for Transient Analysis. North Holland, Amsterdam, pp. 157–219.
Piperno, S., 1997. Explicit/implicit fluid/structure staggered procedures with a structural predictor & fluid subcycling for 2D inviscid aeroelastic simulations. Int. J. Numer. Meth. Fluids 25, 1207–1226.
Rapaport, D.C., 1995. The Art of Molecular Dynamics Simulation. Cambridge University Press.
Schlick, T., 2000. Molecular Modeling & Simulation. An Interdisciplinary Guide. Springer-Verlag, New York.
Schrefler, B.A., 1985. A partitioned solution procedure for geothermal reservoir analysis. Commun. Appl. Numer. Meth. 1, 53–56.
Stillinger, F.H., Weber, T.A., 1985. Computer simulation of local order in condensed phases of silicon. Phys. Rev. B 31, 5262–5271.
Tabor, D., 1975. Interaction between surfaces: adhesion & friction. In: Blake, Y (Ed.), Surface Physics of Materials, vol. II. Academic Press, New York (Chapter 10).
Tai, Y.-C., Noelle, S., Gray, J.M.N.T., Hutter, K., 2002. Shock capturing & front tracking methods for granular avalanches. J. Comput. Phys. 175, 269–301.
Tai, Y.-C., Gray, J.M.N.T., Hutter, K., Noelle, S., 2001a. Flow of dense avalanches past obstructions. Ann. Glaciol. 32, 281–284.
Tai, Y.-C., Noelle, S., Gray, J.M.N.T., Hutter, K., 2001b. An accurate shock-capturing finite-difference method to solve the Savage–Hutter equations in avalanche dynamics. Ann. Glaciol. 32, 263–267.

Tersoff, J., 1988. Empirical interatomic potential for carbon, with applications to amorphous carbon. Phys. Rev. Lett. 61, 2879–2882.
Wieland, M., Gray, J.M.N.T., Hutter, K., 1999. Channelized free-surface flow of cohesionless granular avalanches in a chute with shallow lateral curvature. J. Fluid Mech. 392, 73–100.
Zienkiewicz, O.C., 1984. Coupled problems & their numerical solution. In: Lewis, R.W., Bettes, P., Hinton, E. (Eds.), Numerical Methods in Coupled Systems. Wiley, Chichester, pp. 35–58.
Zohdi, T.I., 2002. An adaptive-recursive staggering strategy for simulating multifield coupled processes in microheterogeneous solids. Int. J. Numer. Meth. Eng. 53, 1511–1532.
Zohdi, T.I., 2004. Modeling & simulation of a class of coupled thermo-chemo-mechanical processes in multiphase solids. Comput. Meth. Appl. Mech. Eng. 193 (6–8), 679–699.
Zohdi, T.I., 2003a. Large-scale statistical inverse computation of inelastic accretion in transient granular flows. Int. J. Nonlinear Mech. 8 (38), 1205–1219.
Zohdi, T.I., 2003b. Computational design of swarms. Int. J. Numer. Meth. Eng. 57, 2205–2219.
Zohdi, T.I., 2003c. Genetic optimization of statistically uncertain microheterogeneous solids. Philos. Trans. Roy. Soc.: Math. Phys. Eng. Sci. 361 (1806), 1021–1043.
Zohdi, T.I., in press. A computational framework for agglomeration in thermo-chemically reacting granular flows. Proceedings of the Royal Society.